

N69-11426

# CASE FILE COPY

FINAL REPORT

Contract No. NSR 05-264-002

November 1968

EARTH SCIENCE RESEARCH

FINAL REPORT

Contract No. NSR 05-264-002

November 1968

SHAPE AND INTERNAL STRUCTURE OF MOON,  
FROM LUNAR ORBITER DATA

for

NATIONAL AERONAUTICS AND SPACE ADMINISTRATION  
LUNAR ORBITER PROGRAM OFFICE

BY

Donald L. Lamar

and

J. V. McGann-Lamar

EARTH SCIENCE RESEARCH CORPORATION  
P.O. Box 5427  
Santa Monica, California 90405  
Area Code 213 - 395-4528

PREFACE

This report presents the results of a study of the shape and internal structure of the Moon utilizing data from the Lunar Orbiter Program under NASA Contract No. NSR 05-264-002. It is planned to submit the report, less appendix, for consideration for publication in ICARUS.

### SUMMARY

The distribution of continents and maria and the displacement of the Moon's center of figure from the center of mass indicate that the average elevation of continents is greater than that of maria. Comparison of the terms in a spherical harmonic expansion of the lunar gravity field with similar terms in distributions of highlands (continents and areas not within circular basins) reveals that the gross shape, as reflected in the distribution of highlands, is unrelated to the gravity field. Consideration of the  $C_{2,0}$ ,  $C_{2,2}$ , and  $C_{3,0}$  terms in the gravity field and of the distribution of surface features indicates that excess mass underlies the maria and circular basins. Density variations and internal structures which would produce the observed gravity field are calculated for (1) a rigid Moon with a random lumpiness and (2) a Moon in isostatic equilibrium. The density contrasts and dimensions for each model are equally probable. Orbiter data are insufficient to determine the overall moment of inertia and whether the Moon is homogeneous or differentiated.

ACKNOWLEDGMENTS

The authors wish to express their appreciation to Paul M. Merifield of Earth Science Research Corporation for his valuable assistance in the preparation of this paper. Discussions with Don E. Wilhelms, Desiree Stuart-Alexander and Keith Howard of the U.S. Geological Survey on the results of their studies of the Moonwide distribution of circular basins and maria were of great assistance in the preparation of Figures 1 and 2. The authors are, however, solely responsible for any errors in these figures and the interpretations presented in the text.

CONTENTS

PREFACE . . . . .	iii
SUMMARY . . . . .	iv
ACKNOWLEDGMENTS . . . . .	v
INTRODUCTION . . . . .	1
RELATIVE ELEVATION OF CONTINENTS AND MARIA . . . . .	2
DISTRIBUTION OF CONTINENTS, MARIA, AND CIRCULAR BASINS . . . . .	9
LUNAR GRAVITY FIELD . . . . .	13
ORIENTATION OF PRINCIPAL AXES . . . . .	15
MOMENT OF INERTIA . . . . .	18
INTERNAL STRUCTURE . . . . .	19
CONCLUSIONS . . . . .	25
REFERENCES . . . . .	26
APPENDIX . . . . .	28

## INTRODUCTION

Analyses of tracking data from the U.S. Lunar Orbiter series of spacecraft (Michael, et al., 1967; Tolson and Gapcynski, 1967; Michael, 1967; Lorell and Sjogren, 1968) and the Soviet Luna-10 (Akim, 1966) have yielded values for the coefficients of a spherical harmonic expansion of the external lunar gravity field. Lunar Orbiter photographs of the backside provide Moonwide data on the distribution of continents, maria, and circular basins (Lunar Farside Charts LFC-1 and LFC-2, 1967). Determinations of the lunar radius by image motion study of Lunar Orbiter photographs (Michael, 1967) and radar observations (Shapiro et al., 1967) have yielded additional information on the relationship between the Moon's center of figure and center of mass. Because of this increased knowledge, it is appropriate to reconsider the relationships between the Moon's gravitational field, internal structure, shape, and the distribution of gross surface features discussed previously (Lamar and McGann, 1966a).

### RELATIVE ELEVATION OF CONTINENTS AND MARIA

Determinations of the lunar radius by analysis of ranger impacts (Sjogren and Trask, 1965), image motion study of Lunar Orbiter photographs (Michael, 1967), and radar observations (Shapiro, et al., 1967) have yielded values which are inconsistent with the elevations shown on the charts of the Aeronautical Chart and Information Center (ACIC), U.S. Air Force, St. Louis. The origin of coordinates for the charts is a mean sphere which best fits the center of volume, whereas the origin for the other determinations is the center of mass. Thus it has been suggested (Sjogren, 1966; Michael, 1967; Shapiro, et al., 1967) that the discrepancies may be the result of displacement between the Moon's center of figure and center of mass.

The relationship between the center of figure and center of mass must be known to accurately determine the relationships between the gravity field, shape and internal structure. For such studies it will be necessary to prepare contour maps showing elevations with respect to the Moon's center of mass. The Moon's gross shape has been approximated on the assumption of a systematic difference in elevation between continents and maria (Lamar and McGann, 1966a). In their analysis of the relationships between the Earth's shape, gravity field and internal structure, Munk and MacDonald (1960a) followed a similar approach by assuming a systematic difference in elevation between continents and ocean basins.

Lamar and McGann (1966a) suggested that the average elevation (relative to the center of mass) of the continents is 3 km greater than the maria. Goudas (1966) questioned this assumption, pointing out that recent stereoscopic elevation determinations reveal no such relationship. The origin of coordinates for these elevations is a mean sphere which best fits the points or the center of volume. The relationship between the center of volume and center of mass must be known before any systematic difference in elevation between continents and maria can be established from stereoscopic observations.

The problem may be visualized by imagining that the Earth lacks oceans, which provide a convenient level surface centered on the Earth's

center of mass. An observer on the Moon studying the Earth's shape by stereoscopic methods or observations of the limb would logically choose the Earth's center of volume as the origin of coordinates. If our lunar observer viewed the Earth with the center of the Pacific Basin on one limb, the center of the Pacific Basin would have about the same elevation as continental areas on the Earth's opposite side, relative to a coordinate system with its origin at the center of the Earth's disk or center of volume.

Similarly in the case of the Moon, it is possible that the continents are systematically higher relative to the center of mass and that some maria surfaces, relative to the center of figure, are higher than some continental areas. Therefore, it will not be possible to use the stereoscopic height determinations to establish any systematic Moonwide difference in elevation between continents and maria until such observations are transformed so that the origin of coordinates is the center of mass. The authors (Lamar and McGann, 1966a,b) were thus incorrect in stating that Hedervari's analysis of Baldwin's (1961, 1963) data was pertinent, and the relative accuracy of stereoscopic determinations by different investigators discussed by Goudas (1966) has no bearing on the problem.

As pointed out by O'Keefe and Cameron (1962) prior to the Ranger and Lunar Orbiter programs, the Moon's center of disk was known to be situated about 1 km south of the center of mass. O'Keefe and Cameron made a least squares solution to determine the sphere which most nearly fits the coordinates determined from stereoscopic observations cataloged by Schrutka-Rechtenstamm (1958). The origin of Schrutka-Rechtenstamm's coordinates is a center of disk derived from limb observations.

O'Keefe and Cameron found that the center of the mean sphere has the following coordinates with respect to the origin:  $y = -0.4 \pm 0.4$  km and  $z = -1.4 \pm 0.4$  km where the x axis points to the Earth, y points east, and z is the north polar axis. Their analysis indicates that the center of the mean sphere, fitting the stereoscopic observations, should lie about 2 km south of the center of mass. This displacement of the center of figure from the center of mass is consistent with the higher proportion of continental areas in the southern hemisphere

compared to the northern hemisphere (Fig. 1 and 2) and with a systematic excess in elevation of continents over maria. Although the east-west separation is small and uncertain, the apparent direction of separation is opposite of what would be expected from the greater proportion of continental areas in the western hemisphere and from an excess in elevation of continents over maria.

Analysis of tracking data from the Ranger flights to the Moon (Sjogren and Trask, 1965) and the first photographs (Lipskii, 1961) of the Moon's farside provided the first indication that a relationship analogous to that between the north and south hemispheres exists between the Moon's farside and Earth-facing hemispheres. The farside pictures indicate that there is a much smaller percentage of maria on the farside than on the hemisphere facing the Earth. If a systematic difference in elevation between continents and maria exists, the Moon's center of figure relative to the center of mass should be displaced away from the Earth. Tracking of the Ranger spacecraft revealed that the radius from the center of mass is about 3 km less than the value indicated on the ACIC charts (Sjogren and Trask, 1965). Since the origin of coordinates for these charts is based on a mean sphere determined from stereoscopic observations, the Ranger data indicate that the center of figure is displaced away from the Earth. This displacement could have been predicted from the relative absence of maria on the farside and the assumption of a systematic excess in elevation of the continents over maria.

Preliminary determinations of the Moon's radius with respect to the center of mass in the equatorial region facing the Earth have been accomplished by analysis of image motion on pictures taken by Lunar Orbiter (Michael, 1967). This investigation also revealed that the radii are systematically lower by 1 to 3 km (average about 2 km) than the radii on the curve obtained from harmonic analysis of the ACIC selenodetic control system by Bray and Goudas (1966). Measurements of the lunar radius, made by combining radar determinations of the distance to sub-earth points on the Moon, and range data of Lunar Orbiter 1 and 2 also produced values about 1 to 2 km less than the radii determined from the stereoscopic observations (Shapiro, et al., 1967). Thus the

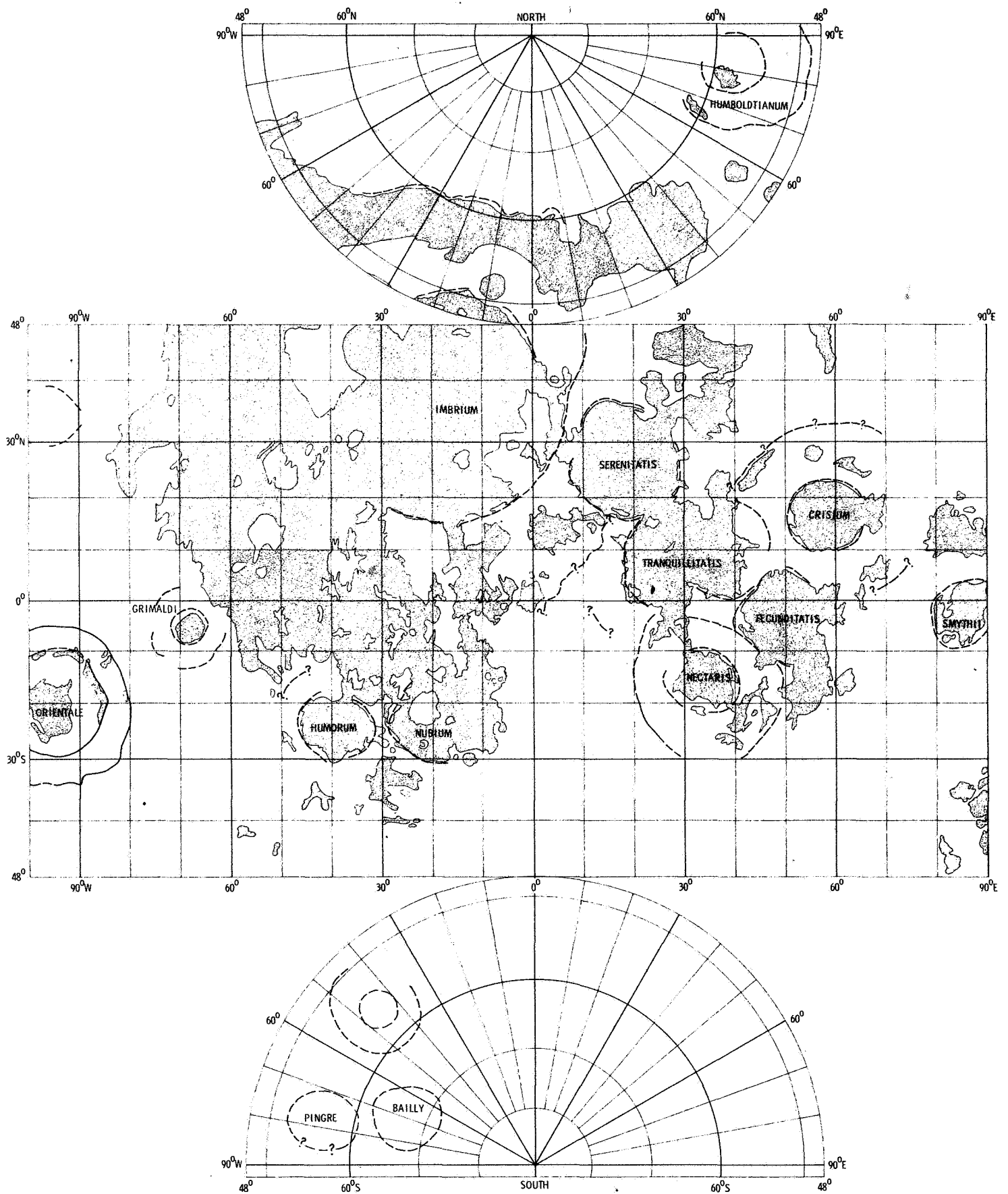


Fig. 1 Earth-facing side of the Moon showing distribution of continents, mare, and circular basins.

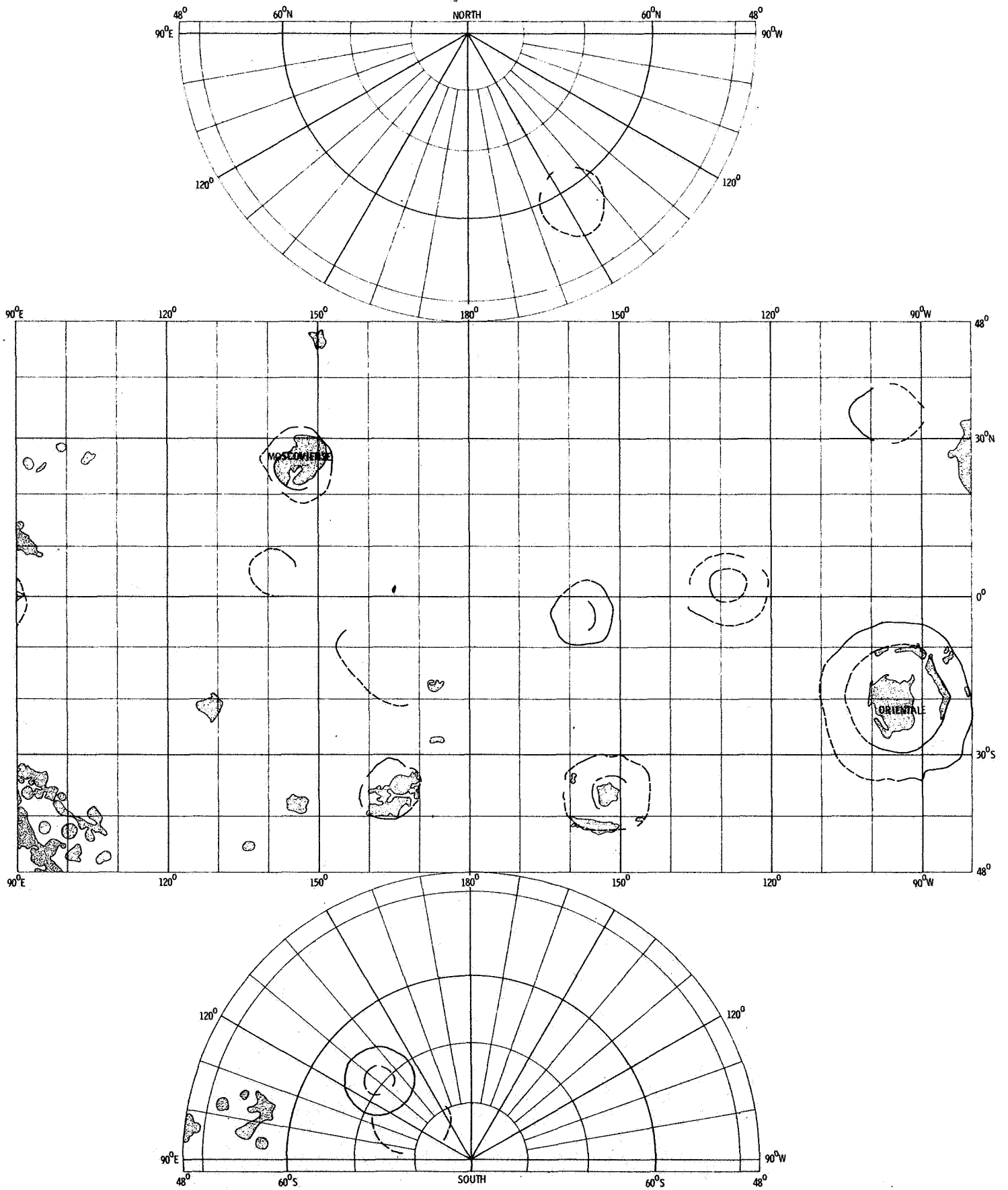


Fig. 2 Farside of the Moon showing distribution of continents, mare, and circular basins.

analysis of data from the Lunar Orbiters substantiates the hypothesis of a systematic excess of elevation of continental areas over maria, which is related to a displacement of the center of figure from the center of mass.

As shown in Fig. 3, if a systematic difference in elevation, amounting to  $H$ , exists between continents and maria on opposite hemispheres, then the displacement between the center of mass and center of disk is  $H/2$ . The displacement of the center of mass 1 km north of the center of disk on the Earth-facing hemisphere is consistent with the higher percentage of continental areas in the Moon's southern hemisphere and with a systematic difference in elevation of about 3 km.

The displacement of about 2 km between the Earthward and farside hemispheres (corresponding to  $H/2$  on Fig. 3) leads to an unexpectedly high estimate of about 5 km for the excess in elevation of continents over maria ( $H$  on Fig. 3). However, the radii determinations by image motion are concentrated in the equatorial region (Michael, 1967), which is predominantly maria; thus the relative percentage of maria on the Earthward side may be overemphasized. The existing data appear to establish that continents are systematically higher than maria relative to the Moon's center of mass. Additional studies are required to determine the magnitude of this difference and to learn the average depth of the circular basins.

As previously noted (Lamar and McGann, 1966a), if the Moon's density distribution is spherically symmetrical, then to a first approximation the orientation of the axes of the principal moments of inertia would be related to distribution of continents, low-lying maria, and circular basins. Low-lying areas would be concentrated in polar regions and around an axis in the equatorial plane at  $90^{\circ}$ - $270^{\circ}$  east longitude.

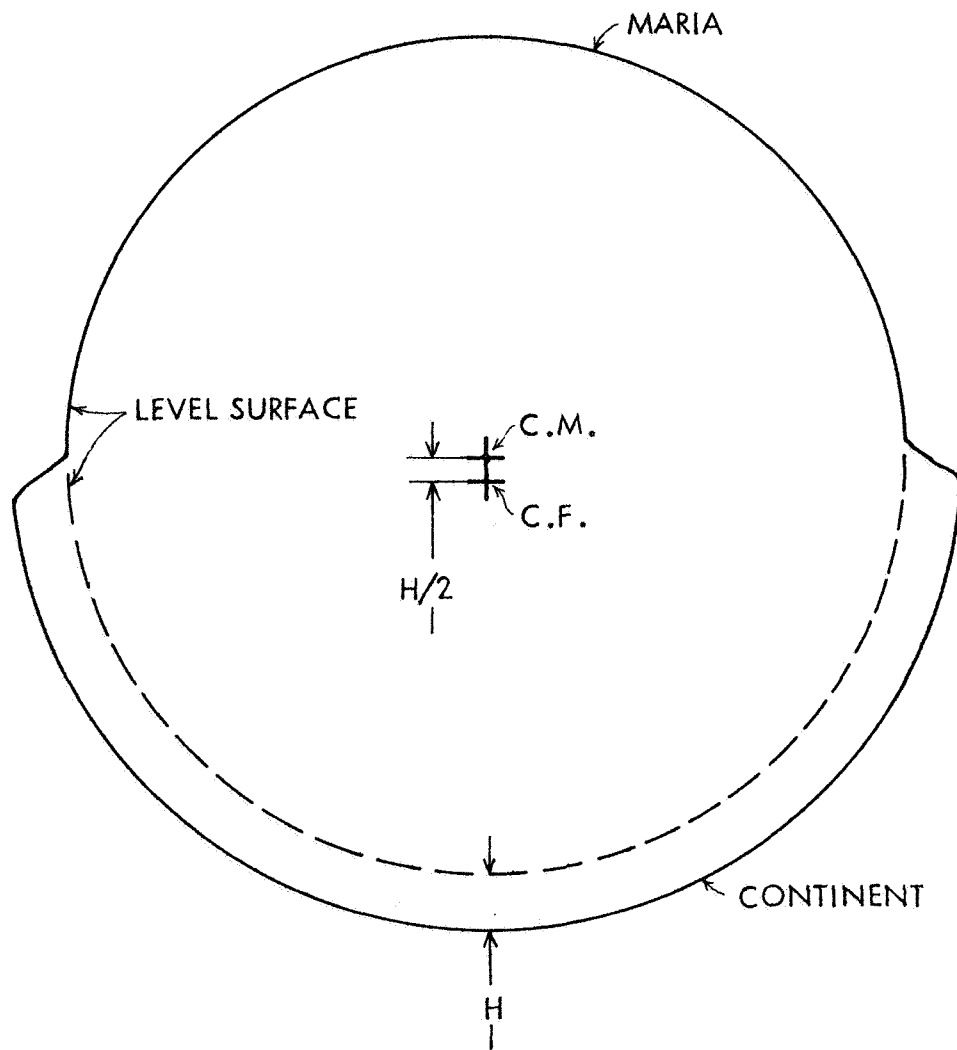


Fig. 3 Relationship between center of mass (c.m.) and center of figure (c.f.) for concentration of maria and continents in distinct hemispheres. A systematic excess in elevation (H) of continents over maria with respect to a level surface is assumed.

### DISTRIBUTION OF CONTINENTS, MARIA, AND CIRCULAR BASINS

Figures 1 and 2 show the Moonwide distribution of continents, maria, and circular basins greater than 300 km in diameter. The maps were compiled from the USAF Lunar Reference Mosaic (1960), the USAF Project Apollo Lunar Planning Chart (1962), Whitaker, et al. (1963), Lunar Farside Chart LFC-1 (1967), and by study of Lunar Orbiter photographs. These maps indicate that the Moonwide distribution of low-lying maria and circular basins is the opposite of that required to explain the orientation of the axes of principal moments of inertia. That is, low-lying maria and circular basins appear to be concentrated in equatorial regions and around an axis in the equatorial plane at  $0^{\circ}$ - $180^{\circ}$  east longitude.

In order to determine the orientation of the principal axes of the distribution of gross surface features and models of internal structure, it is convenient to express the distribution of surface features in terms of the coefficients of spherical harmonic representations of functions analogous to the ocean function of the Earth presented by Munk and MacDonald (1960b). A computer program utilizing the equations presented by Munk and MacDonald was used to calculate coefficients of spherical harmonic expansions for distributions of gross surface features. Because the expansion used by Munk and MacDonald is different from the expansion of the gravity field in spherical harmonics given below, each coefficient in the functions was multiplied by  $(n-m)!/n!$  to permit direct comparison with similar terms in the gravity field.

In calculating the coefficients, the proportion of the surface feature considered was tabulated for squares 10 degrees on each side from Fig. 1 and 2. The values of the coefficients are listed on Table I. Distribution 1 represents a continentality (or non-maria) function. The coefficients of Distribution 2 express the distribution of areas not within the outer rim of a circular basin. In defining the area within a circular basin, questioned outer rims were ignored and incomplete rings were completed.

Muller and Sjogren (1968) have shown that the most youthful appearing circular basins on the nearside (Imbrium, Serenitatis, Crisium,

n m	C' <sub>n,m</sub>				S' <sub>n,m</sub>			
	Dist. 1	Dist. 2	Dist. 3	Dist. 4	Dist. 1	Dist. 2	Dist. 3	Dist. 4
2 0	0.146	0.0841	0.0442	0.0259	-	-	-	-
1 1	-0.0994	-0.0852	-0.0753	-0.0322	0.0309	-0.0238	-0.00882	-0.0157
2 2	-0.0228	-0.0233	-0.0133	-0.00581	0.0282	-0.0178	-0.000306	-0.00612
3 0	0.104	0.0179	0.0362	0.0257	-	-	-	-
1 1	0.0274	-0.0178	-0.0370	-0.00749	0.00335	0.0196	0.00428	0.000342
2 2	-0.00943	-0.0171	-0.0235	-0.0108	0.00768	0.00661	0.0110	-0.000499
3 3	0.00599	0.00124	-0.00192	-0.000845	0.00382	-0.00697	-0.00399	-0.00185
4 0	-0.00377	-0.0256	0.00303	0.0101	-	-	-	-
1 1	0.0129	0.00326	-0.00265	0.00757	-0.00267	0.0152	0.0218	0.0177
2 2	-0.00283	-0.00477	-0.00898	-0.00407	0.00335	0.0131	0.0108	0.00330
3 3	0.00078	-0.00216	-0.00195	-0.000917	-0.00043	0.00253	0.00327	0.000544
4 4	0.00098	0.000290	0.000080	0.0000092	0.00023	0.000263	0.000084	0.000098
5 0	0.0125	0.140	0.0936	0.0254	-	-	-	-
1 1	0.00298	0.0241	0.0295	0.0196	-0.0143	-0.0280	-0.000272	-0.00302
2 2	-0.00195	0.000388	0.000342	0.00106	-0.000021	-0.000734	-0.00152	0.00101
3 3	-0.00050	-0.00105	-0.000645	-0.000502	0.00016	0.00183	0.000930	0.000292
4 4	0.00011	0.000027	0.000012	-0.000030	-0.00023	0.000124	0.000240	0.000050
5 5	0.000068	0.000080	0.000023	0.000016	-0.0000078	0.000030	0.000034	0.000020
6 0	-0.0415	-0.0206	-0.0671	-0.0920	-	-	-	-
7 0	-0.00167	-0.0550	-0.0804	-0.0488	-	-	-	-
8 0	-0.0423	0.00485	0.00861	-0.00886	-	-	-	-

Table I - Coefficients of spherical harmonic representations of surface features.  
Nature of distributions given in text.

Humorum, and Nectaris) and Orientale Basin on the limb caused perturbations in the motions of Lunar Orbiters. They suggest the perturbations are due to excess mass beneath these basins. Comparison of the outlines of the gravity anomalies shown on their map with Fig. 1 indicates that the excess masses are concentrated within the inner rings of the Imbrium and Nectaris Basins. For the Crisium and Humorum Basins, the existence of an outer rim or ring relative to the excess mass concentration is not certain. In the case of the Serenitatis Basin, the existence of an outer ring is not clear. A suggestion of an outer rim appears along the northeast shore of Lacus Somniorum and the south shore of Mare Vaporum and the area to the southeast along the Hyginus Rille.

Desiree Stuart-Alexander and Keith Howard (personal communications, 1968) have made a preliminary study of the relative ages of circular basins greater than 300 km in diameter on the basis of (a) ratio of basin size to size of larger superposed craters, (b) sharpness of scarp, (c) presence of rim deposits, (d) completeness of outer ring, (e) circularity, (f) completeness of an inner ring, and (g) subjective rank of overall age. Based on their analysis, Serenitatis is the oldest of the nearside basins which perturbs the motions of the Lunar Orbiters. They consider the following additional basins to be younger than Serenitatis: Grimaldi, Bailly, Moscoviense, and unnamed basins identified by the coordinates of their centers, 45W, 55S; 140E, 5N; 165E, 35S; 130E, 70S; 155W, 5S; and 130W, 5N. Distribution 3 represents the areas outside of the outer rims of circular basins as young as Serenitatis.

In considering the significance of the inner and outer rings or rims, it is important to note that the development of the inner ring appears to be dependent on the diameter of the outer ring. For example, in the following small basins younger than Serenitatis, the inner ring is absent: Bailly; 140E, 5N; and 165E, 35S. For the following slightly larger basins younger than Serenitatis, the inner ring is indistinct or incomplete compared to the outer rim: Moscoviense; 130E, 70S; and 155W, 5S. Therefore, in considering the distribution of areas outside of inner rings, single-ringed basins were ignored. Distribution 4 represents areas outside of the inner rings of the basins which Muller

and Sjogren (1968) suggest are underlain by excess mass, and the following additional basins: Grimaldi; Moscoviense; 45W, 55S; 130E, 70S; 155W, 5S; 130W, 5N.

Because of variations in illumination, the tone of flat lying areas differs with different photos and the precise distribution of maria is difficult to determine. The outlines of the circular basins are also commonly obscured. Although the distribution of gross surface features shown on Fig. 1 and 2 may be modified by more detailed studies, the values of the coefficients in Table I should not change significantly with subsequent analysis of improved maps.

# LUNAR GRAVITY FIELD

The lunar gravitational potential function is expressed as the following series expansion in spherical harmonics with coefficients  $C_{n,m}$  and  $S_{n,m}$ :

$$U = \frac{\mu}{r} \left[ 1 + \sum_{n=2}^{\infty} \sum_{m=0}^n \frac{a^n}{r^n} P_{n,m}(\sin \phi) (C_{n,m} \cos m\lambda + S_{n,m} \sin m\lambda) \right]$$

where  $\mu$  is the product of the gravitational constant and the mass of the moon,  $r$  is the radial distance from the center of the moon,  $a$  is the mean radius of the moon,  $P_{n,m}$  are associated Legendre polynomials,  $\phi$  is the latitude, and  $\lambda$  is the longitude. This is the form of the potential recommended by the International Astronomical Union and has been adopted in analyses of the Lunar Orbiter tracking data (Michael, *et al.*, 1967; Tolson and Gapcynski, 1967; Michael, 1967; Lorell and Sjogren, 1968). The values of the coefficients in the gravity field presented by Lorell and Sjogren (1968), Tolson and Gapcynski (1967), and Akim (1966) with the correction in sign of the terms with odd value of  $m$ , suggested by Tolson and Gapcynski (1967), are presented on Table II.

It is interesting to note that in all three analyses the  $C_{2,1}$  term departs significantly from zero. In Lorell and Sjogren's (1968) analysis, the  $S_{2,2}$  term also departs from zero. Jeffreys (1962, p. 141) pointed out that the lack of a wobble of the Moon's axis of rotation indicates that the  $C_{2,1}$  and  $S_{2,1}$  terms in the gravity field must be very nearly zero or no more than 0.001 of the  $C_{2,2}$  and  $S_{2,2}$  terms. If the  $S_{2,2}$  term is not very close to zero, then the resulting torque should cause the Moon to rotate until the line pointing toward the Earth is a principal axis and this term vanishes. According to Michael (1967), the  $C_{2,1}$ ,  $S_{2,1}$ , and  $S_{2,2}$  coefficients have tended to decrease as additional tracking data have been analyzed. It is possible that, with sufficient data and further analyses, these terms will completely vanish.

n	m	$C_{n,m} \times 10^{-4}$			$S_{n,m} \times 10^{-4}$		
		Akim (1966)	Tolson and Gapcynski (1967)	Lorell and Sjogren (1968)	Akim (1966)	Tolson and Gapcynski (1967)	Lorell and Sjogren (1968)
2	0	-2.06 ± .22	-2.0596 ± .141	-2.0263 ± .0143	-	-	-
	1	-.157 ± .059	-.1661 ± .051	-.0878 ± .0131	-.0361 ± .0358	.0080 ± .039	.0150 ± .0139
	2	.140 ± .012	.2042 ± .029	.2191 ± .0249	-.0139 ± .0145	-.0342 ± .025	.1310 ± .0335
3	0	-.363 ± .099	-.3773 ± .180	-.2223 ± .0262	-	-	-
	1	.568 ± .026	.3012 ± .048	.3636 ± .0025	.178 ± .032	.1762 ± .053	.0740 ± .0032
	2	.118 ± .047	.1294 ± .028	-.0257 ± .0058	-.00702 ± .046	-.0147 ± .033	-.0200 ± .0063
	3	-	.0317 ± .015	-.0265 ± .0079	-	-.0043 ± .018	-.0496 ± .0114
4	0	.333 ± .270	.0798 ± .128	.0941 ± .0190	-	-	-
	1	-	-.1560 ± .036	-.1236 ± .0046	-	.0391 ± .028	.0564 ± .0051
	2	-	.0011 ± .010	.0361 ± .0034	-	.0072 ± .013	.0051 ± .0035
	3	-	-.0082 ± .008	.0164 ± .0021	-	-.0001 ± .006	-.0276 ± .0015
	4	-	-.0007 ± .003	.0091 ± .0011	-	.0011 ± .003	.0079 ± .0011
5	0	-	-.5505 ± .171	-.1614 ± .0321	-	-	-
	1	-	-.0385 ± .037	-	-	.0829 ± .031	-
	2	-	.0342 ± .009	-	-	-.0203 ± .008	-
	3	-	-.0071 ± .002	-	-	-.0078 ± .002	-
	4	-	-.0008 ± .001	-	-	-.0013 ± .001	-
	5	-	-.0003 ± .0002	-	-	.0003 ± .0002	-
6	0	-	-	-.1089 ± .0121	-	-	-
7	0	-	-	.1734 ± .0122	-	-	-
8	0	-	-	-.2011 ± .0114	-	-	-

Table II - Gravity Field of Moon Determined from Lunar Orbiters  
(Tolson and Gapcynski, 1967; Lorell and Sjogren, 1968)  
and Luna-10 (Akim, 1966).

# ORIENTATION OF PRINCIPAL AXES

A Cartesian set of coordinate axes fixed in the Moon are defined with the x and y axes in the equatorial plane, the x axis directed toward the mean direction to the Earth, and the z axis directed north along the axis of rotation. The second degree terms in the gravity field are related to the moments and products of inertia as follows:

$$\begin{aligned} I_{xx} &= A & I_{xy} &= 2Ma^2 S_{2,2} \\ I_{yy} &= B = A + 4Ma^2 C_{2,2} & I_{xz} &= Ma^2 C_{2,1} \\ I_{zz} &= C = A + Ma^2 (2C_{2,2} - C_{2,0}) & I_{yz} &= Ma^2 S_{2,1} \end{aligned}$$

where A, B, and C are the Moon's principal moments of inertia, M is the Moon's mass, and a is the Moon's mean radius.

The second degree terms in the spherical harmonic representation of the distribution of surface features are related to the moments and products of inertia as follows:

$$\begin{aligned} I_{xx} &= \frac{8\pi}{3} \sigma a^4 \left[ C'_{0,0} + \frac{1}{10} C'_{2,0} - \frac{3}{5} C'_{2,2} \right] & I_{xy} &= \frac{8\pi}{5} \sigma a^4 S'_{2,2} \\ I_{yy} &= \frac{8\pi}{3} \sigma a^4 \left[ C'_{0,0} + \frac{1}{10} C'_{2,0} + \frac{3}{5} C'_{2,2} \right] & I_{xz} &= \frac{4\pi}{5} \sigma a^4 C'_{2,1} \\ I_{zz} &= \frac{8\pi}{3} \sigma a^4 \left[ C'_{0,0} - \frac{1}{5} C'_{2,0} \right] & I_{yz} &= \frac{4\pi}{5} \sigma a^4 S'_{2,1} \end{aligned}$$

where  $\sigma$  is the load per unit area due to the higher elevation of continents and areas outside of circular basins.

The orientations of the principal axes of the continent distribution, the non-circular basin distributions, and the overall mass distribution expressed by the gravity potential coefficients indicated in Table III were determined by the above equations and the equations presented by Munk and MacDonald (1960b). The east longitudes of the axes of least and greatest moments of inertia in the equatorial plane

	Maximum moment of inertia		Intermediate moment of inertia		Minimum moment of inertia		Minimum moment of inertia in equatorial plane
	$\lambda$	$\phi$	$\lambda$	$\phi$	$\lambda$	$\phi$	
Akim (1966)	16.0	176.0	273.1	91.0	3.0	86.1	2.8
Tolson and Gapcynski (1967)	353.5	176.1	274.6	89.3	4.7	86.2	4.8
Lorell and Sjogren (1968)	354.1	178.0	74.6	89.7	344.6	88.0	344.6
Distribution 1	17.3	109.2	278.6	113.3	322.8	31.0	295.5
Distribution 2	349.9	114.3	271.4	66.1	40.1	35.3	71.3
Distribution 3	2.8	112.5	275.6	85.6	12.4	32.9	89.3
Distribution 4	355.0	118.7	279.1	66.0	42.5	39.0	66.8

Table III - Orientations of principal axes determined from lunar gravity field and coefficients of spherical harmonic representations of distributions of surface features;  $\lambda$  is east longitude and  $\phi$  is co-latitude in degrees.

related to the gravity field and the spherical harmonic representations of surface features were determined by  $\tan 2\lambda = S_{2,2}/C_{2,2}$ . The east longitudes corresponding to the axes of least moment of inertia on Table III were identified as representing the smaller value of the quantity:  $-C_{2,2} \cos 2\lambda - 2S_{2,2} \sin 2\lambda$ .

For stable orientation, the axis of greatest moment of inertia corresponds to the rotational axis and the axis of least moment lies along a line pointing to the Earth. The orientations of the principal axes, determined from the coefficients in the gravity field presented by Akim (1966) and Tolson and Gapcynski (1967), lie within 5 degrees of the stable orientation. For the coefficients presented by Lorell and Sjogren (1968), the axes lie within about 15 degrees of the stable orientation. The principal axes of the distributions of surface features are within 30 to 40 degrees of an orientation opposite to a stable orientation. That is, the axes of least moment of inertia lie within 40 degrees of the polar axis and the axes of greatest moment are within 30 degrees of the center of the disk. These orientations and the lower elevation of maria and circular basins verify the authors' earlier rejection of a homogeneous density distribution within the Moon. The effect of an excess load ( $\sigma$ ) due to the greater elevation of continents and areas outside of circular basins is more than compensated for by excess mass beneath the maria and circular basins.

Significantly, Nash (1963) suggested that excess mass beneath the maria may be the explanation for the relative lack of maria on the Moon's farside. Nash hypothesized that the Moon was locked into synchronous rotation, with excess mass beneath the maria facing the Earth in a stable orientation. He also suggested that the maria resulted from the impact of objects denser than the Moon and that the apparent concentration of maria in the plane of the ecliptic may be explained by an asteroidal origin for the impacting objects. However, any process of maria formation which is random and leads to an excess of mass beneath the maria surface could result in the present distribution of maria with respect to the Moon's rotational axis and the direction to the Earth. The present distribution could be the result of wander of the Moon's axes to the position of stable equilibrium, regardless of the original cause of the density distribution.

MOMENT OF INERTIA

Tolson and Gapcynski (1967) have calculated the value of the quantity  $q = 3C/2Ma^2 = 0.5895 \pm 0.05$  where  $C$  is the moment of inertia about the axis of rotation from their values of  $C_{2,0}$  and  $C_{2,2}$ . According to Jeffreys (1962), for a chemically homogeneous moon with increase in density with depth due to internal pressure,  $q = 0.596$ . According to our calculations (Lamar and McGann, 1966a) for a linear increase in density from  $3.2 \text{ gm/cm}^3$  below a thin crust to  $3.76 \text{ gm/cm}^3$  at the center,  $q = 0.592$ , and for a more extreme differentiated model in which the density increases linearly from  $2.8 \text{ gm/cm}^3$  at the surface to  $5.0 \text{ gm/cm}^3$  at the center,  $q = 0.568$ . The problem of the overall moment of inertia has been considerably improved by the orbiter data and it is apparently no longer necessary to consider the possibility that the density of the Moon decreases with depth. However the data are still insufficient to decide whether the Moon is differentiated or chemically homogeneous.

### INTERNAL STRUCTURE

In this section we consider internal density distributions which reconcile the coefficients of spherical harmonic expansions of the external gravity field with similar coefficients representing surface feature distributions. Arbitrary cutoffs are assumed between maria and continents and between circular basins and areas outside of circular basins. If such models reflected the true internal structure, the principal axes of the distributions of highlands (continents and areas outside of circular basins) would correspond to the Moon's principal axes. If excess mass beneath the maria or circular basins is greater than the load due to the higher elevation of continents and areas outside of basins, the Moon's axis of least moment of inertia will correspond to the axis of greatest moment for the distribution of highlands.

As noted in the previous section for the distributions considered, the principal axes of the surface features are no closer than 30 to 40 degrees to such an orientation. Because of this, and the preliminary nature of the coefficients of the gravity field, consideration of more elaborate models of internal structure is not now justified. Eventually it will be appropriate to consider models of internal structure in which the mass effects beneath individual basins is considered a function of the age and size of the feature. If the principal axes for such models correspond to the Moon's principal axes, it would be of interest to consider higher order terms in the gravity field and distribution of surface features.

In the present analysis, only the terms which reflect the oblateness ( $C_{2,0}$ ), ellipticity of the equator ( $C_{2,2}$ ), and north-south asymmetry ( $C_{3,0}$ ) are considered. The calculations give an idea of the internal density variations required to reconcile the gravity field and the gross shape as reflected in the distribution of surface features. The following models of internal structure are considered:

(1) The Moon is assumed to be a rigid body not in isostatic equilibrium; the density variations are assumed to be the result of random inhomogeneities as suggested by Urey, Elsasser, and Rochester (1959).

(2) The Moon is assumed to be in isostatic equilibrium, and differences in elevation are assumed to be compensated for by variations in crustal thickness as suggested by O'Keefe and Cameron (1962). For this model the required density variations beneath the crust could be due to temperature differences related to thermal convection in the mantle, as proposed by Kopal (1962) and Runcorn (1962). From Jeffreys (1962, p. 182) the equation for the gravitational potential of a surface distribution over a sphere of radius  $R$  is

$$U = \frac{4\pi G \sigma R}{(2n+1)} \sum_{n=2}^{\infty} \sum_{m=0}^n \left(\frac{R}{r}\right)^{n+1} P_{n,m}(\sin \phi) (C'_{n,m} \cos m\lambda + S'_{n,m} \sin m\lambda)$$

where  $G$  is the gravitational constant,  $\sigma$  is the surface area density over the sphere expressed in a spherical harmonic representation with coefficients  $C'_{n,m}$  and  $S'_{n,m}$ , and  $r$  is the distance from the center of the sphere. From the equation for the lunar gravitational potential, we derive the following expression for the effects on individual coefficients of the gravity field:

$$C_{n,m} = \frac{4\pi \sigma R^{n+2} C'_{n,m}}{(2n+1) M a^n}$$

where  $M$  is the mass and  $a$  is the Moon's mean radius.

Assuming the Moon is homogeneous and substituting the expression for the mass of a homogeneous sphere, we derive

$$H = d_{n,m} a/3$$

where  $H$  is the height of a surface layer,  $a$  is the Moon's mean radius (1738 km), and  $d_{n,m}$  is  $(2n+1)$  times the ratio of the coefficient in the gravity field to a similar term in the distribution of the surface layer. The surface layer is assumed to have the same density as the Moon. Table IV shows the excess elevation ( $H$ ) of maria and circular basins required to produce the gravity field determined by Tolson and Gapcynski (1967) from the distributions of surface features. However,

the available data indicate that maria and circular basins are low in elevation, thus these calculations indicate that the assumption of a homogeneous density distribution is false.

	Dist. 1	Dist. 2	Dist. 3	Dist. 4
$C_{2,0}$	4.1	7.1	13.5	23.1
$C_{2,2}$	2.6	2.5	4.5	10.2
$C_{3,0}$	1.5	8.5	4.2	6.0

Table IV - Excess elevation (km) of maria and circular basins required to produce coefficients in the lunar gravity field determined by Tolson and Gapcynski (1967) from distributions of surface features and a homogeneous Moon.

To estimate simple mass distributions which will produce the values of terms in the gravity field, it is necessary to derive general equations analogous to those presented in an earlier paper for the second order terms (Lamar and McGann, 1966a). In integral form the effect on individual coefficients in the gravity field is

$$C_{n,m} = \frac{3C'_{n,m}}{(2n+1)\rho_a a^{n+3}} \int_0^{a+H} r^{n+2} \Delta\rho(r) dr$$

where H is the assumed excess elevation of continents and areas outside of circular basins,  $\rho_a$  is the Moon's average density (3.33 gms/cm<sup>3</sup>), and  $\Delta\rho(r)$  is the excess in density of material beneath maria and circular basins.

For a rigid, lumpy model, we assume a linear decrease in the density contrast with depth, or  $\Delta\rho(r) = \Delta\rho(a)(r/a)$ , where  $\Delta\rho(a)$  is the density contrast at the surface; by integration

$$\Delta\rho(a) = \rho_a \left[ \frac{d_{n,m}}{3} - \frac{H}{a} \right] (n+4)$$

It is assumed that the density of material near the surface is equal to the average density of the Moon.

For the extreme case of a rigid, lumpy model, we assume that maria and circular basins are directly underlain by a layer of nickel-iron. The thickness ( $t$ ) of the layer is found to be

$$t = \frac{\rho_a}{(\rho_i - \rho_a)} \left[ H - \frac{d_{n,m} a}{3} \right]$$

where  $\rho_i$  is the density of nickel iron ( $7.8 \text{ gm/cm}^3$ ).

If topographic irregularities are assumed to be compensated for by variations in thickness of crust floating on mantle, we assume zero thickness for crust beneath maria and circular basins, compensation at depth,  $D$ , and a density excess in mantle beneath circular basins and maria which decreases linearly with depth; by integration

$$\Delta\rho(a) = \frac{(n+4)}{\left[1 - (n+4) \frac{D}{a}\right]} \left[ \frac{\rho_a d_{n,m}}{3} - (\rho_c - \rho_m) \frac{D}{a} - \rho_c \frac{H}{a} \right]$$

where  $\rho_c$  is the density of crustal material and  $\rho_m$  is the density of the mantle directly beneath maria and circular basins. We assume a condition of zero stress at the Moon's center; from Lamar and McGann (1966a)

$$\Delta\rho(a) = \frac{3}{\left(1 - 3 \frac{D}{a}\right)} \left[ \rho_c \frac{H}{a} - (\rho_m - \rho_c) \frac{D}{a} \right]$$

We assume that the average density of crustal material is  $2.8 \text{ gm/cm}^3$  and that the density contrast between the crust and mantle ( $\rho_m - \rho_c$ ) is  $0.4 \text{ gm/cm}^3$ . Accepted values for the Earth are  $\rho_c = 2.84 \text{ gm/cm}^3$  and  $(\rho_m - \rho_c) = 0.43 \text{ gm/cm}^3$  (Worzel and Shurbet, 1955). For the second order terms and the relations

$$C_{2,0} = -J_2^0 = \frac{1}{Ma^2} \left[ \frac{A+B}{2} - C \right], \quad C'_{2,0} = a_2^0$$

$$C_{2,2} = -J_2^2 = \frac{1}{4Ma^2} (B - A), \quad C'_{2,2} = \frac{1}{2} a_2^2$$

$$\beta = \frac{C - A}{B} = \frac{C - A}{C}, \quad \gamma = \frac{B - A}{C}, \quad C = \frac{2}{5} Ma^2$$

where C, B, and A are the principal moments of inertia of the Moon, the above equations reduce to those presented in Lamar and McGann (1966a).

Table V lists values of parameters for the models of internal structure calculated by the above equations from the coefficients for distributions of surface features and Tolson and Gapcynski's (1967) determination of the gravity field.

		Rigid Models			Isostatic Model	
		H (km)	Density contrast, $\Delta\rho$ (a) (gm/cm <sup>3</sup> )	Thickness of Nickel-Iron Layer, t (km)	Density Contrast, $\Delta\rho$ (a) (gm/cm <sup>3</sup> )	Depth of Compensation, D (km)
Dist. 1	C <sub>2,0</sub>	3.0	0.081	5.3	0.017	44.3
		5.0	0.10	6.8	0.018	58.5
	C <sub>2,2</sub>	3.0	0.064	4.2	0.011	35.7
		5.0	0.087	5.7	0.011	49.9
	C <sub>3,0</sub>	3.0	0.060	3.3	0.0064	29.8
		5.0	0.087	4.8	0.0066	43.9
Dist. 2	C <sub>2,0</sub>	3.0	0.12	7.5	0.032	62.0
		5.0	0.14	9.0	0.033	76.5
	C <sub>2,2</sub>	3.0	0.064	4.1	0.011	35.4
		5.0	0.087	5.6	0.011	49.6
	C <sub>3,0</sub>	3.0	0.15	8.6	0.042	73.8
		5.0	0.18	10.1	0.044	88.6
Dist. 3	C <sub>2,0</sub>	3.0	0.19	12.3	0.068	101.7
		5.0	0.21	13.8	0.071	116.9
	C <sub>2,2</sub>	3.0	0.086	5.6	0.019	46.5
		5.0	0.11	7.0	0.020	60.7
	C <sub>3,0</sub>	3.0	0.097	5.4	0.019	46.5
		5.0	0.12	6.9	0.020	60.8
Dist. 4	C <sub>2,0</sub>	3.0	0.30	19.4	0.015	169.6
		5.0	0.32	20.9	0.016	187.4
	C <sub>2,2</sub>	3.0	0.15	9.8	0.048	80.7
		5.0	0.17	11.3	0.050	95.5
	C <sub>3,0</sub>	3.0	0.12	6.7	0.028	57.3
		5.0	0.15	8.2	0.029	71.8

Table V - Parameters for models of internal structure required to produce coefficients in the lunar gravity field determined by Tolson and Gapcynski (1967) from distributions of surface features. The quantity H represents assumed values of the excess elevation of continents and areas outside of circular basins.

### CONCLUSIONS

An excess in density beneath the lowlands (maria and circular basins) is indicated by the relation between the  $C_{2,0}$ ,  $C_{2,2}$ , and  $C_{3,0}$  terms in the gravity field and the distribution of surface features (Table V). However, the density excesses corresponding to the three terms differ by no more than a factor of three for the three models of internal structure considered.

Distribution 4 most closely corresponds to the existence of "mascons" beneath the inner rims of the most youthful appearing circular basins, as revealed by the analysis of Muller and Sjogren (1968). If mascons are assumed to be masses of nickel-iron, they correspond to a layer averaging about 12 km thick, as determined from Table V, or more realistically, a layer several tens of kilometers in thickness with a 10-20% excess of nickel-iron.

The isostatic model fits the data equally well. The required depths of compensation for this model appear reasonable; they are not significantly greater than corresponding depths determined for the Earth. The required excess in the density of the mantle beneath circular basins and maria for the isostatic model could be explained by a lower temperature of a few hundred degrees centigrade.

Data from the Lunar Orbiter Program have greatly improved our knowledge of the Moon's gravity field and gross shape as reflected in the distribution of surface features. However, these data alone are insufficient to determine which model of internal structure is most probable, or the nature of the processes which have shaped the Moon's surface.

REFERENCES

- Akim, E. L. (1966) Determination of gravitational field of the Moon from the motion of the artificial lunar satellite Luna 10; translated by J. C. Noyes from: Doklady of the Academy of Sciences of the USSR, Vol. 170, p. 799-802.
- Baldwin, R. B. (1961) A lunar contour map: Sky and Telescope, Vol. 21, p. 84-85.
- Baldwin, R. B. (1963) The Measure of the Moon: Univ. of Chicago Press, Chicago, Illinois, 488 p.
- Bray, T. A. and C. L. Goudas (1966) A contour map based on the selenodetic control system of the A.C.I.C.: Icarus, Vol. 5, p. 526-535.
- Goudas, C. L. (1966) Note on "Shape and Internal structure of the Moon" by Lamar and McGann: Icarus, Vol. 5, p. 99-100.
- Jeffreys, Harold (1962) The Earth, 4th rev. ed.: Cambridge University Press, London, 438 p.
- Kopal, Z. (1962) The internal constitution of the Moon: Planetary Space Sci., Vol. 9, p. 625-638.
- Lamar, D. L. and Jeannine McGann (1966a) Shape and internal structure of the Moon: Icarus, Vol. 5, p. 10-23.
- Lamar, D. L. and Jeannine McGann (1966b) Reply to "Note on the shape and internal structure of the Moon" by C. L. Goudas: Icarus, Vol. 5, p. 101.
- Lipskii, Yu. N. (1961) The photography of the reverse side of the Moon-- techniques and preliminary results: Soviet Astron. - AJ: Vol. 4, p. 976-989.
- Lorell, J. and W. L. Sjogren (1968) Lunar gravity: preliminary estimates from Lunar Orbiter: Science, Vol. 159, p. 625-627.
- Lunar Farside Chart LFC-1 (1967) Aeronautical Chart and Information Center, St. Louis, Missouri.
- Lunar Farside Chart LFC-2 (1967) Aeronautical Chart and Information Center, St. Louis, Missouri.
- Michael, W. H., Jr. (1967) Physical properties of the Moon as determined from Lunar Orbiter data: Presented at the Fourteenth General Assembly of the International Union of Geodesy and Geophysics Meeting, Lucerne, Switzerland, 13 p.
- Michael, W. H., Jr., R. H. Tolson, and J. P. Gapcynski (1967) Preliminary results on the gravitational field of the Moon from analysis of Lunar Orbiter Tracking data: Presented at the American Geophysical Union Annual Meeting, 20 p.

- Muller, P. M. and W. L. Sjogren (1968) Mascons: lunar mass concentrations: Science, Vol. 161, p. 680-684.
- Munk, W. H. and G. J. F. MacDonald (1960a) Continentality and the gravitational field of the Earth: J. Geophys. Res., Vol. 65, p. 2169-2172.
- Munk, W. H. and G. J. F. MacDonald (1960b) The Rotation of the Earth: Cambridge University Press, London, 323 p.
- Nash, D. B. (1963) On the distribution of lunar maria and the synchronous rotation of the Moon: Icarus, Vol. 1, p. 372-373.
- O'Keefe, J. A. and W. S. Cameron (1962) Evidence from the Moon's surface features for the production of lunar granites: Icarus, Vol. 1, p. 271-285.
- Runcorn, S. K. (1962) Convection in the Moon: Nature, Vol. 195, p. 1150-1151.
- Schrutka-Rechtenstamm, G. (1958) Neureduktion der 150 Mondpunkte der Breslauer Messungen von J. Franz; Sitzber. der Osterr. Akad. Wiss., Math.-Naturw. Kl., Abt. II, Vol. 167, p. 71-123.
- Shapiro, A., E. A. Uliana, B. S. Yaplee, and S. H. Knowles (1967) Lunar radius from radar measurements; Presented at COSPAR Assembly, London, England, 23 p.
- Sjogren, W. L. (1966) Estimate of four topocentric lunar radii: Proceedings of the Second International Conference on Selenodesy and Lunar Topography, Manchester, England, 3 p.
- Sjogren, W. L. and D. W. Trask (1965) Results on physical constant and related data from the radio tracking of Mariner (Venus) and Ranger III-VII missions: J. Spacecraft; Vol. 2, p. 689-697.
- Tolson, R. H. and J. P. Gapcynski (1967) An Analysis of the lunar gravitational field as obtained from Lunar Orbiter tracking data: Presented at the IQSY/COSPAR Assemblies, London, England, 22 p.
- Urey, H. C., W. M. Elsasser, and M. G. Rochester (1959) Note on the internal structure of the Moon: Astrophys. J., Vol. 129, p. 842-848.
- USAF Lunar Reference Mosaic (1960) Aeronautical Chart and Information Center, St. Louis, Missouri.
- USAF Project Apollo Lunar Planning Chart (1962) Aeronautical Chart and Information Center, St. Louis, Missouri.
- Whitaker, E. A., G. P. Kuiper, W. K. Hartmann and L. H. Spradley (1963) Rectified Lunar Atlas: The University of Arizona Press, Tucson.
- Worzel, J. L. and G. L. Shurbet (1955) Gravity interpretations from standard oceanic and continental crustal sections: Geol. Soc. Am., Spec. Paper 62, p. 87-100.

## Appendix

### Computer Programs

This appendix contains listings, explanations and flow diagrams for all programs written for this project. The "Spherical Harmonics" program consists of a main routine and two subroutines. "MAIN" assumes the surface of the Moon to be divided into  $10^6$  squares for calculation of the spherical harmonic coefficients of the distribution of surface features. The subroutine "PRNT" produces a table of the distribution of the surface features as determined from maps of the Moon and is the input to the program. The subroutine "TENSr" generates the tensor for computing the moments of inertia about the principal axes, and their orientation. The "Moon Modeling" program computes the parameters for different models of internal structure.

Table 1--Symbols Used in "MAIN" routine of Spherical Harmonics Program

Fortran Nomenclature	Explanation
Variables	
RUN	Label for data identification
THTA	$\theta$ , colatitude
ELAM	$\lambda$ , east longitude
F	$f(\theta, \lambda)$ ; continentality function
ELC $\phi$	$\Delta\lambda$
THC $\phi$	$\Delta\theta$
SITA	$\sin \theta$
C $\phi$ TA	$\cos \theta$
F1	$(m + r)!$
F2	$(n - r)!$
F3	$(n - m - r)!$
F4	$r!$
Q	$(\cos \theta - 1)^{(n-m-r)}$
R	$(\cos \theta + 1)^r$
HASU	$[(\cos \theta - 1)^{n-m-r}(\cos \theta + 1)^r]/[(m + r)!(n - r)!(n - m - r)!r!]$ ; one term of summation
FISU	$\sum_{i=0}^{n-m} \frac{(\cos \theta - 1)^{n-m-r}(\cos \theta + 1)^r}{(m + r)!(n - r)!(n - m - r)!r!}$
F5	$(n - m)!$
F6	$(n + m)!$
SM	$(\sin \theta)^m$
TTN	$2^n$

Table 1--continued

Fortran Nomenclature	Explanation
P	$p_n^m(\cos \theta) = \frac{(n-m)!(n+m)!(\sin \theta)^m}{2^n}$ $\sum_{i=0}^{n-m} \frac{(\cos \theta - 1)^{n-m-r}(\cos \theta + 1)^r}{(m+r)!(n-r)!(n-m-r)!r!}$
SIML	$\sin m\lambda$
CØML	$\cos m\lambda$
THP	$[(p_n^m(\cos \theta)\sin \theta)_1 + (p_n^m(\cos \theta)\sin \theta)_{i+1}]/2.$
APAL	$[(\cos m\lambda)_1 + (\cos m\lambda)_{i+1}]/2.$
BPAL	$[(\sin m\lambda)_1 + (\sin m\lambda)_{i+1}]/2.$
A	$f(\theta,\lambda) \left[ \frac{(p_n^m \sin \theta)_1 + (p_n^m \sin \theta)_{i+1}}{2.} \right] \left[ \frac{(\cos m\lambda)_1 + (\cos m\lambda)_{i+1}}{2.} \right] \Delta\theta\Delta\lambda$
B	$f(\theta,\lambda) \left[ \frac{(p_n^m \sin \theta)_1 + (p_n^m \sin \theta)_{i+1}}{2.} \right] \left[ \frac{(\sin m\lambda)_1 + (\sin m\lambda)_{i+1}}{2.} \right] \Delta\theta\Delta\lambda$
F7	$n!$
CØNST	$(2n+1)n! / 2\pi(n+m)! \quad \text{or}$ $(2n+1)/4\pi$
CSUM	summation of C terms
SSUM	summation of S terms
CNM = CIS	$\left. \begin{matrix} c_{n,m} \\ s_{n,m} \end{matrix} \right\} \begin{matrix} \text{coefficients of a surface spherical harmonic} \\ \text{expansion of the gravity field} \end{matrix}$
SNM = SIS	
Integers	
ICC	number of continentality function distributions to be run
ICCK	run counter
IPRT	switch for requesting printout of table of continentality function
ITR	switch for requesting "TENSr" calculations

Table 1--continued

Fortran Nomenclature	Explanation
NC	number of colatitudes considered
NL	number of east longitudes considered
NMN	number of n,m combinations considered
NMNI	counter for number of n,m combinations
LIM	upper limit for summation
IF1	$(m + r)$
IF2	$(n - r)$
IF3	$(n - m - r)$
IF4	$r$
IF5	$(n - m)$
IF6	$(n + m)$
IF7	$n$

} last term of factorial

Table 2--Symbols Used in "TENSR" subroutine of Spherical Harmonics Program

Fortran Nomenclature	Explanation
Variables	
C00	$C_{0,0}$
C20	$C_{2,0}$
C21	$C_{2,1}$
C22	$C_{2,2}$
S21	$S_{2,1}$
S22	$S_{2,2}$
EM1	$I_{xx}$
EM2	$I_{yy}$
EM3	$I_{zz}$
EM4	$I_{xy}, I_{yx}$
EM5	$I_{xz}, I_{zx}$
EM6	$I_{yz}, I_{zy}$
	} matrix elements
A	Coefficient of $I^3$
B	Coefficient of $I^2$
C	Coefficient of $I$
D	constant term of cubic
Q	} Storage locations used in finding roots of cubic
R	
TEST	
SI	
P	
PART	}
COEF	

Table 2--continued

Fortran Nomenclature	Explanation	
Y1	} storage locations used in finding roots of cubic	
Y2		
Y3		
Z1	} roots of the cubic	
Z2		
Z3		
XP0LE	greatest moment of inertia, $I_x$	
YP0LE	intermediate moment of inertia, $I_y$	
ZP0LE	least moment of inertia, $I_z$	
H1	$\left. \begin{array}{l} I_{xx} - I_x \\ I_{yy} - I_y \\ I_{zz} - I_z \end{array} \right\}$	diagonal terms of orientation matrix
H2		
H3		
X3	$\left. \begin{array}{l} \omega_z/\omega_x \\ \omega_y/\omega_x \\ \omega_x/\omega_x \end{array} \right\}$	direction numbers
X2		
X1		
S1	$\left[ (\omega_z/\omega_x)^2 + (\omega_y/\omega_x)^2 + (\omega_x/\omega_x)^2 \right]^{1/2}$	
CALP1	$\left. \begin{array}{l} \cos \alpha_1 \\ \cos \beta_1 \\ \cos \gamma_1 \end{array} \right\}$	direction cosines
CBET1		
CGAM1		
AML1	$\lambda_1$ ; east longitude (radians) of x-axis	
TTHA1	$\tan \theta_1$	
THA1	$\theta_1$ ; colatitude (radians) of x-axis	
AML11	$\lambda_1$ ; east longitude (degrees) of x-axis	

Table 2--continued

Fortran Nomenclature	Explanation
AML12	$\lambda_1 \pm 180^\circ$
THTA11	$\theta_1$ ; colatitude (degrees) of x-axis
THTA12	$\theta_1 \pm 180^\circ$
(this pattern is repeated for the y and z axes)	
X	$C_{2,2}/S_{2,2}$
Y	$[(C_{2,2}/S_{2,2})^2 + 1]^{1/2}$
TP1	$\tan \phi_1 = C_{2,2}/S_{2,2} + [(C_{2,2}/S_{2,2})^2 + 1]^{1/2}$
PH1	$\phi_1$ ; east longitude (radians)
SPH1	$\sin \phi_1$
CPH1	$\cos \phi_1$
P11	moment of inertia about $\phi_1$
PHI1	$\phi_1$ ; east longitude (degrees)
TP2	$\tan \phi_2 = C_{2,2}/S_{2,2} - [(C_{2,2}/S_{2,2})^2 + 1]^{1/2}$
PH2	$\phi_2$ ; east longitude (radians)
SPH2	$\sin \phi_2$
CPH2	$\cos \phi_2$
P22	moment of inertia about $\phi_2$
PHI2	$\phi_2$ ; east longitude (degrees)
PHMIN	minimum value of moment of inertia

Table 2--continued

Fortran Nomenclature	Explanation
Integers	
ISN	number of sets of spherical harmonic inputs to be run
ISC	run counter
MIN	=1; P11 is a minimum =2; P22 is a minimum

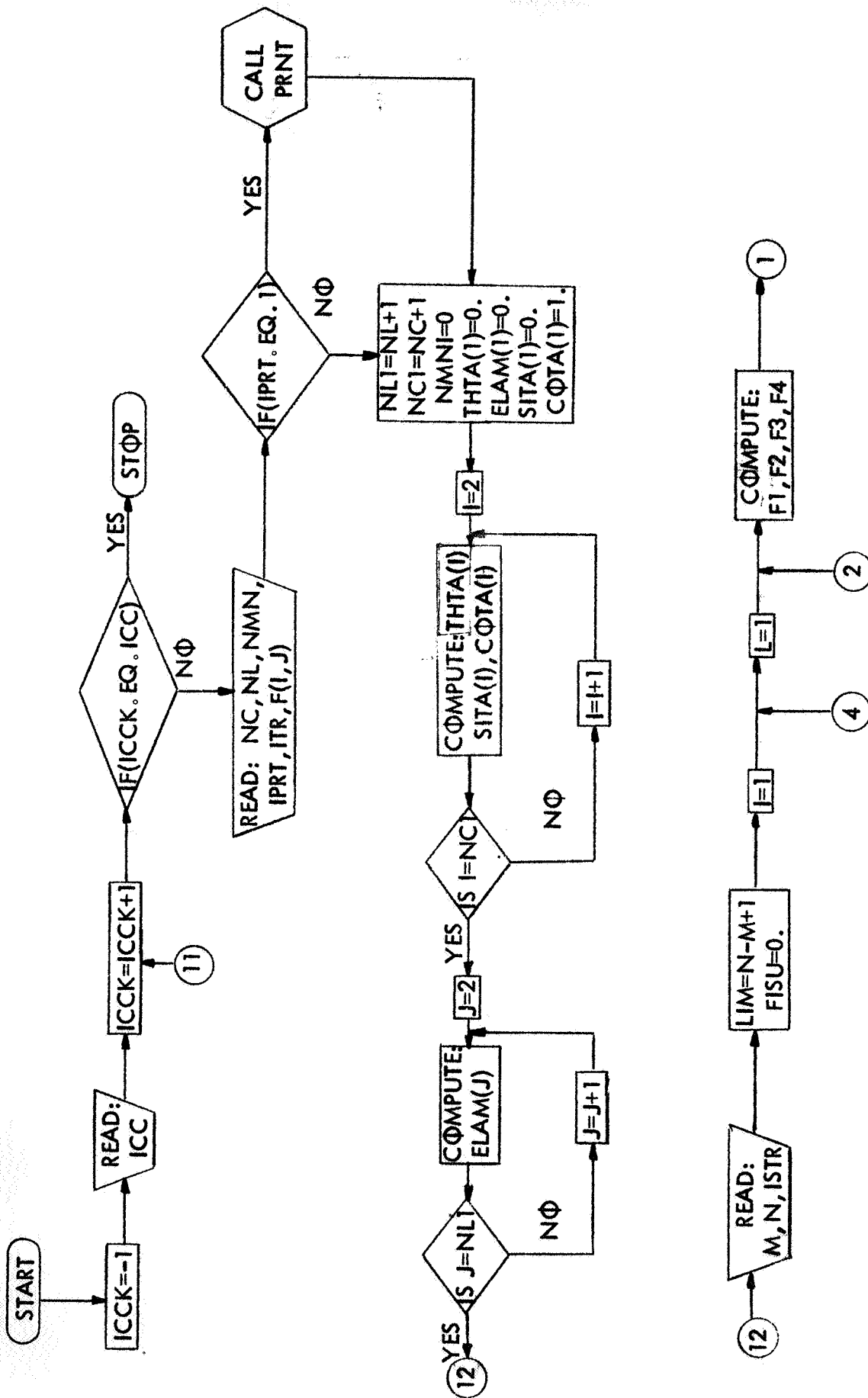


Table 3---Flow Diagram of "MAIN" routine of Spherical Harmonics Program

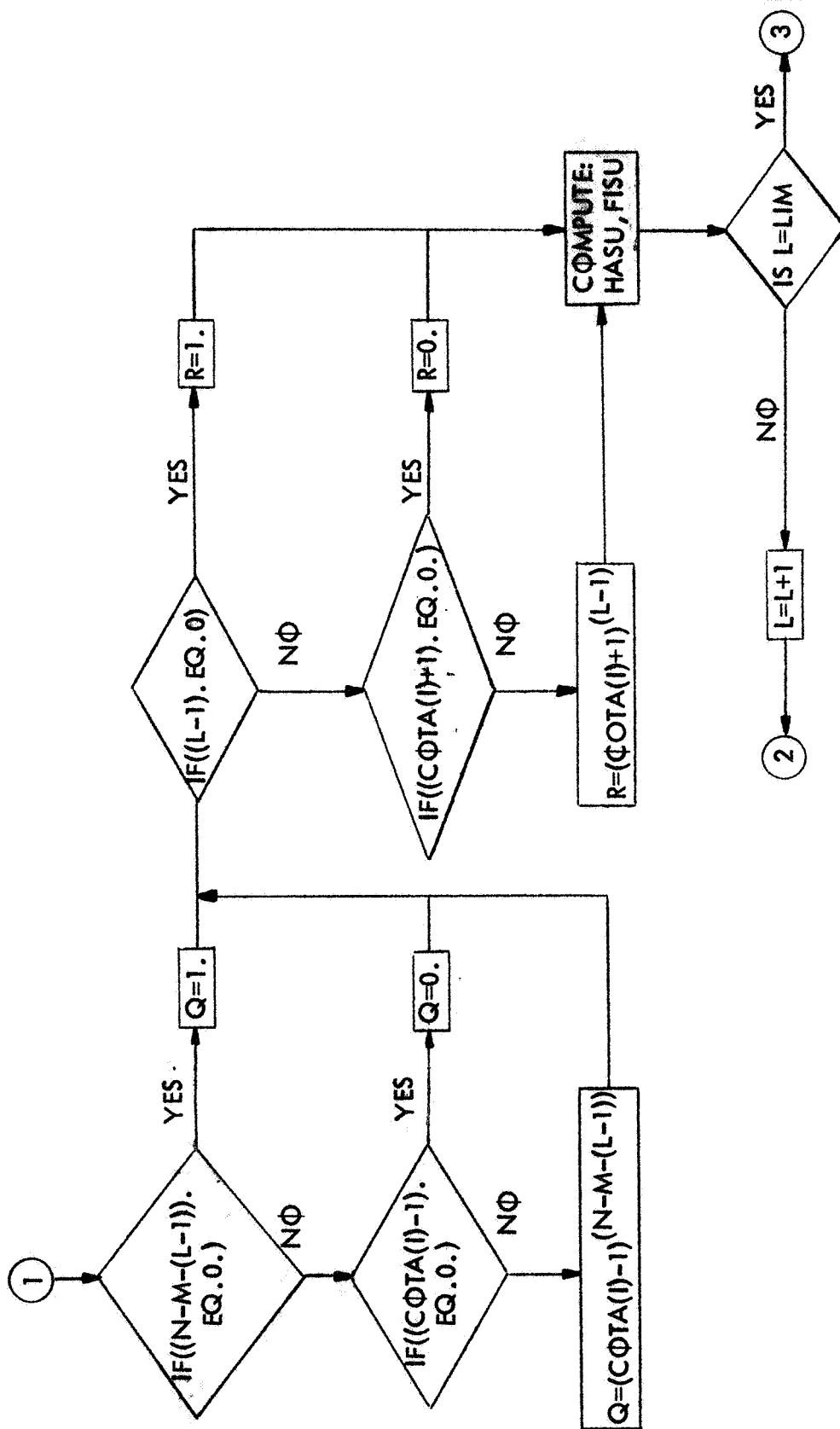


Table 3---Continued

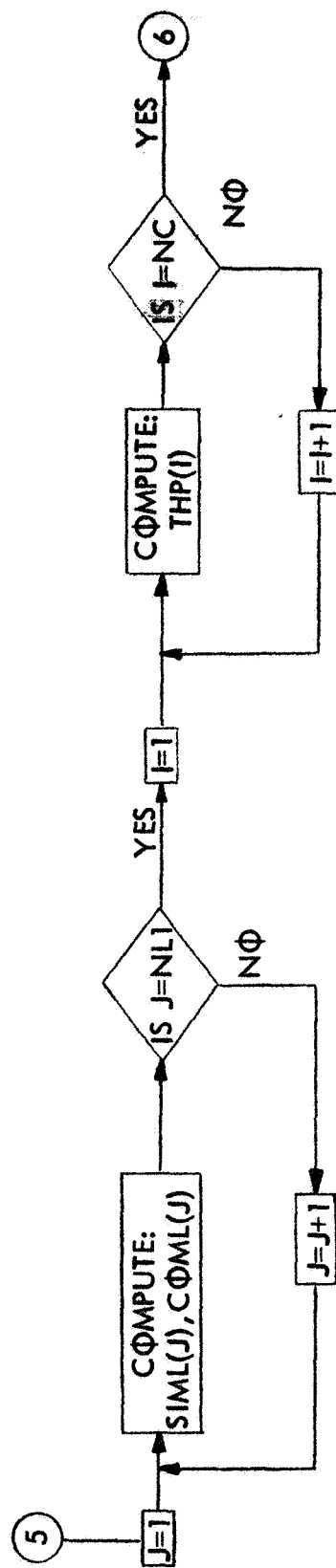
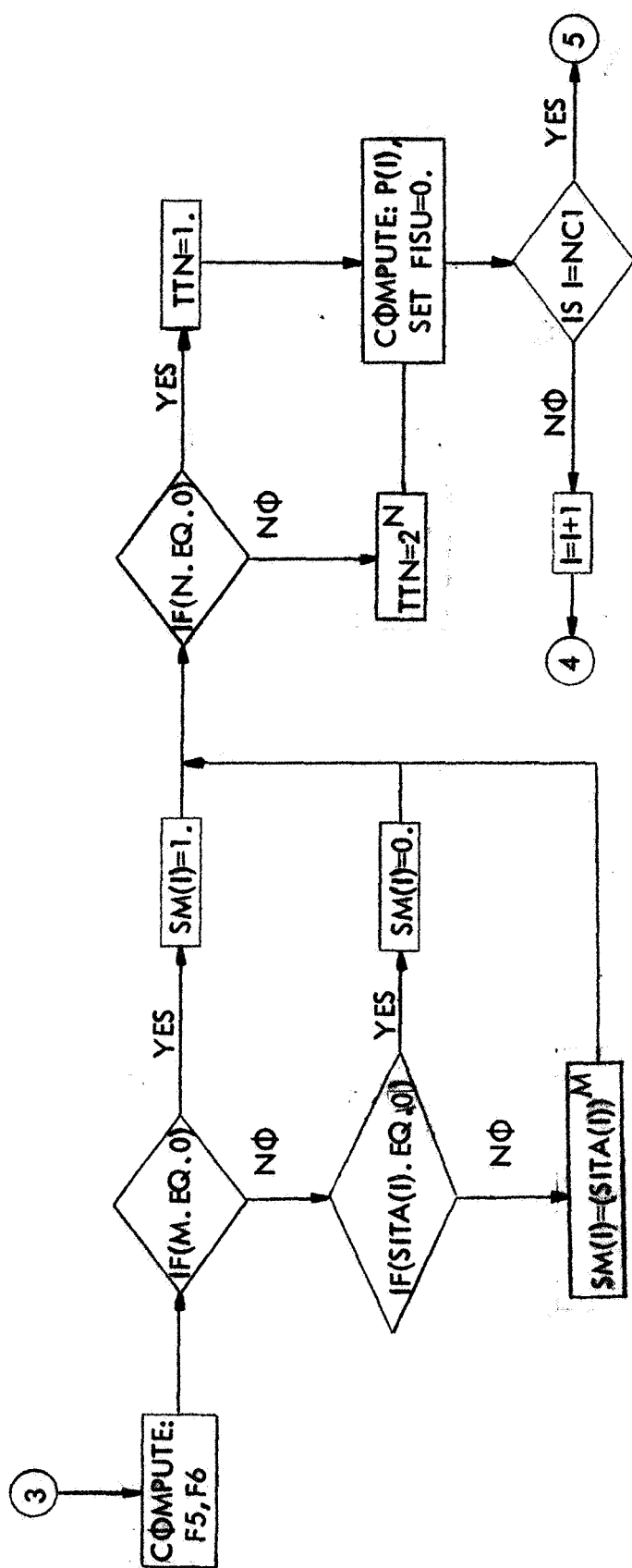


Table 3--Continued

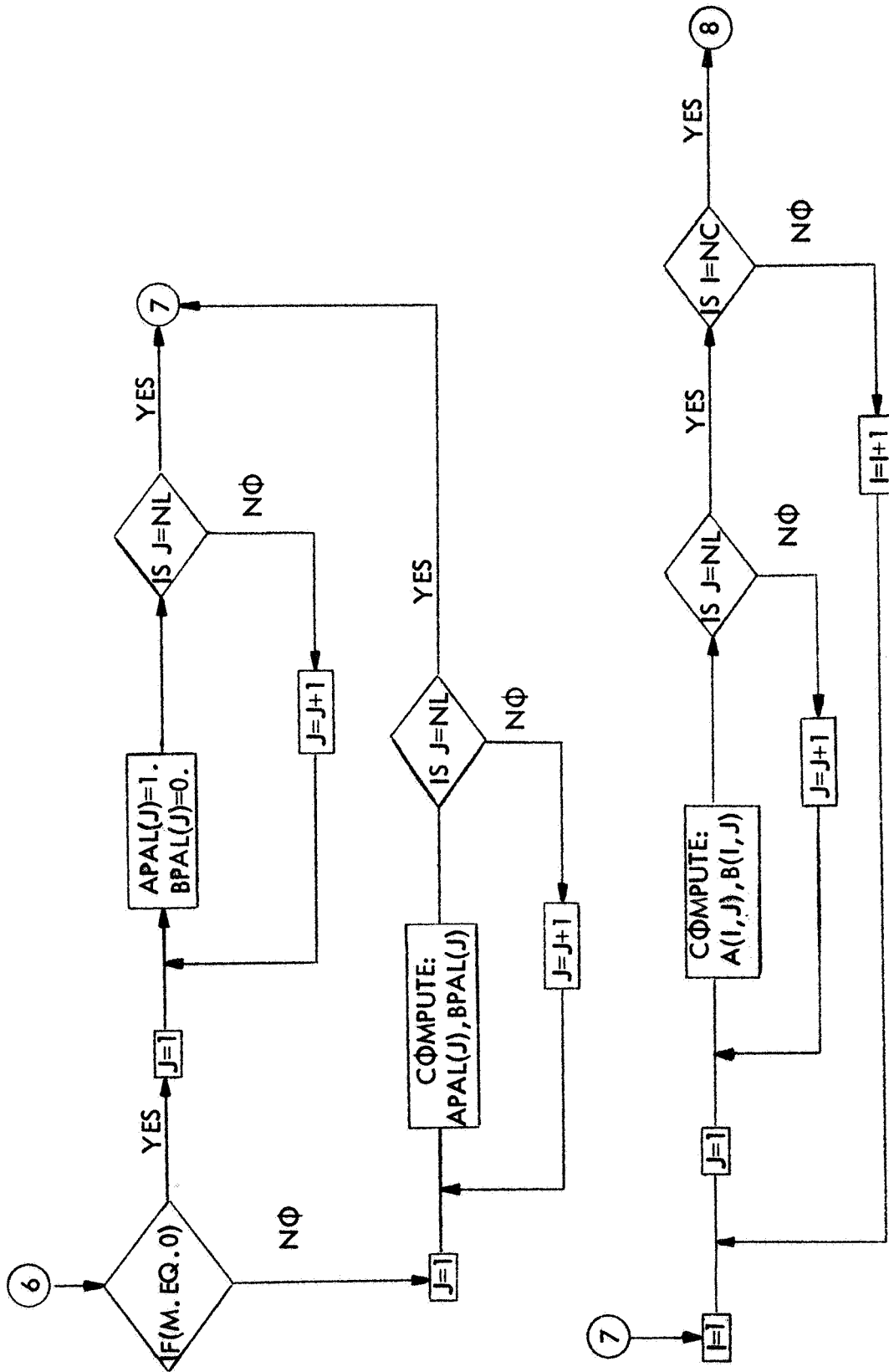


Table 3--Continued

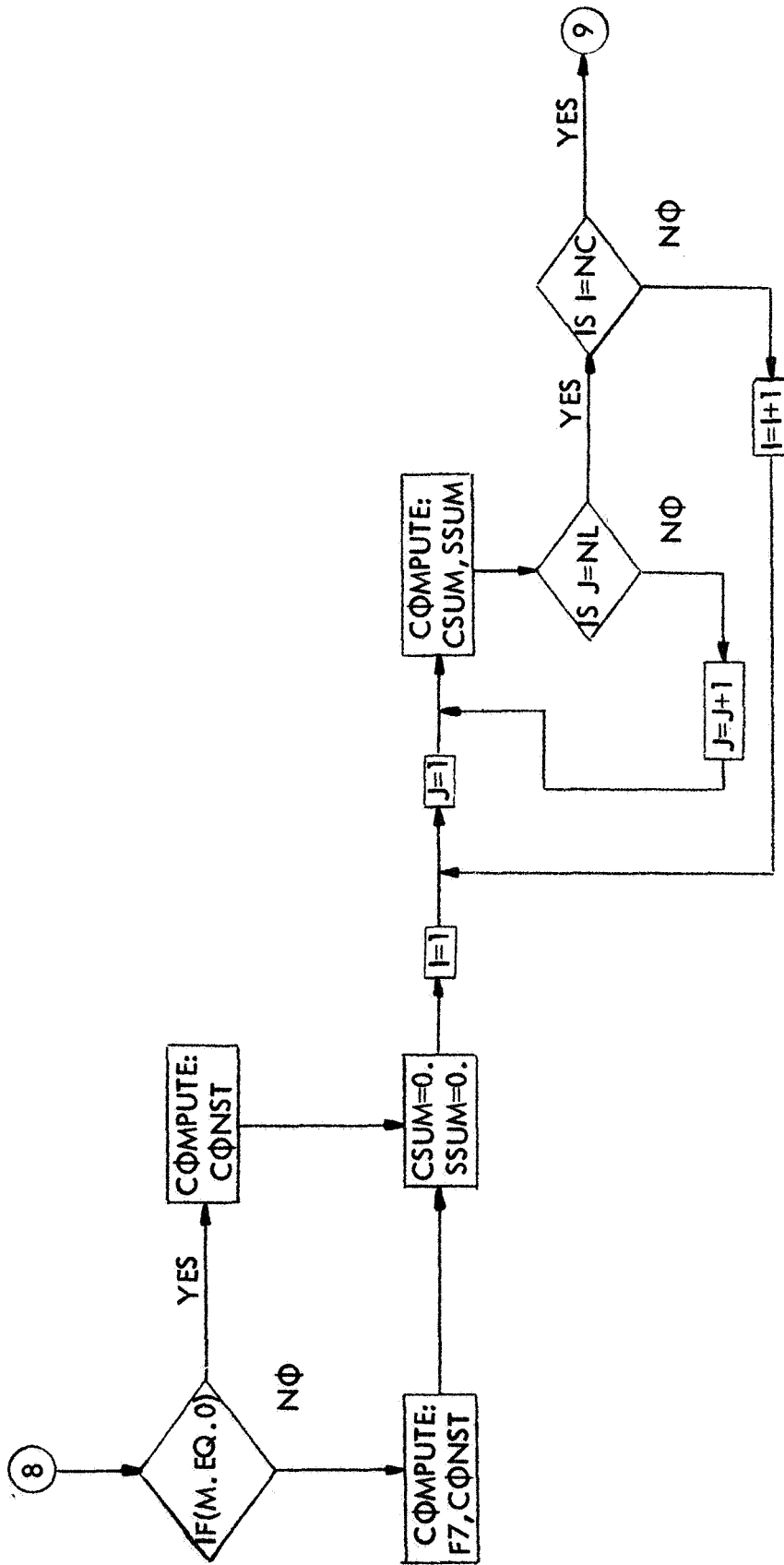


Table 3---Continued

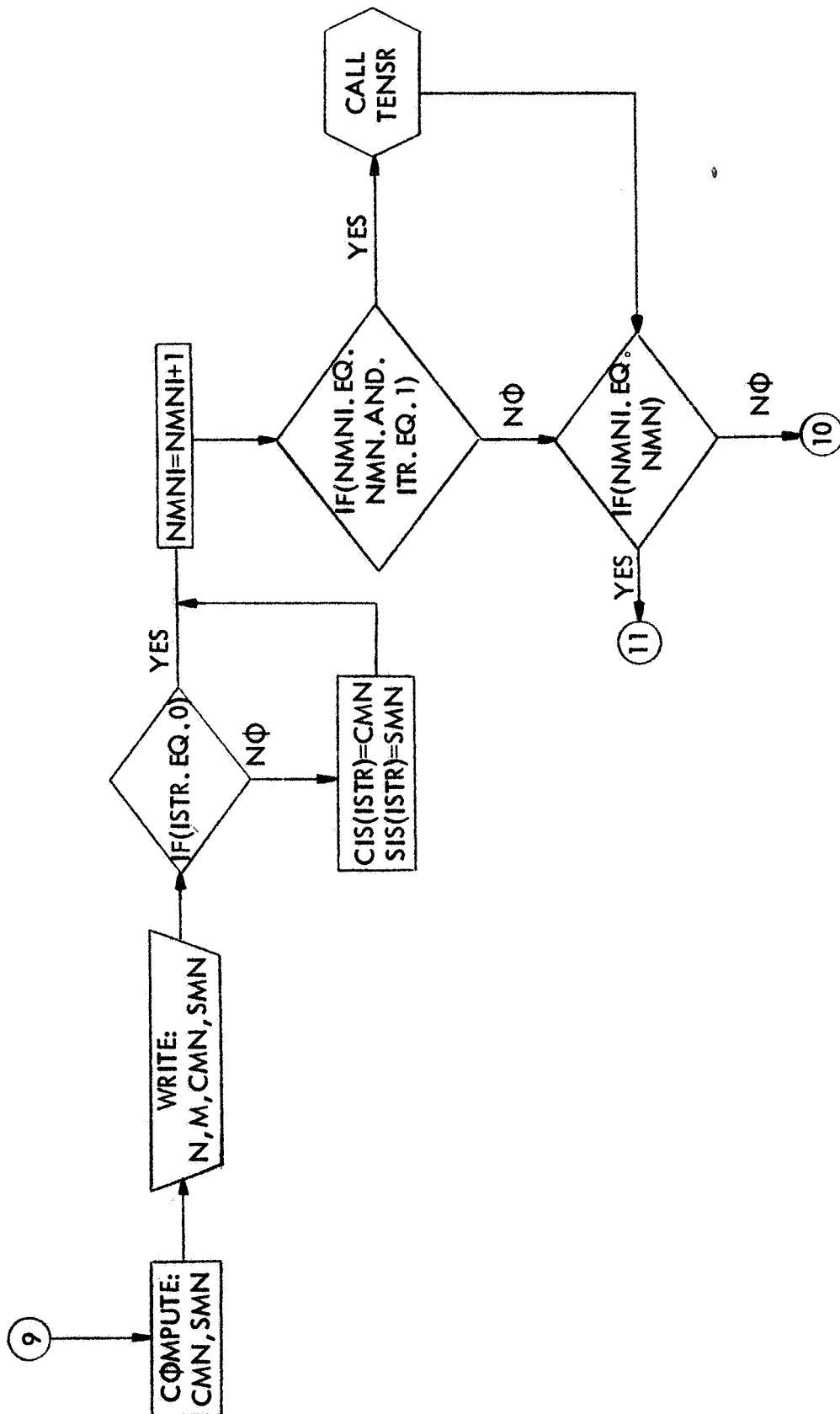


Table 3--Continued

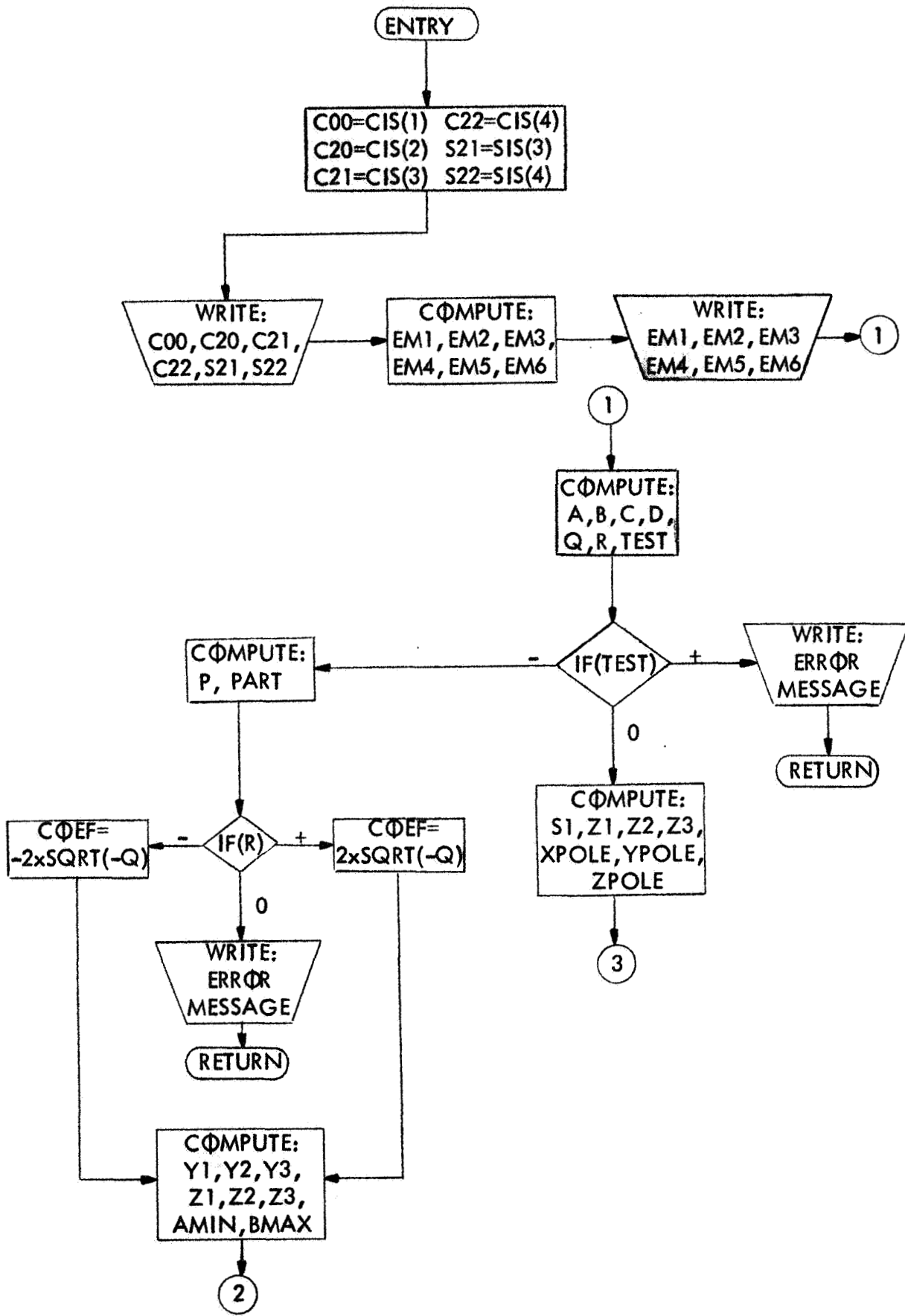


Table 4--Flow Diagram of "TENSr" subroutine of Spherical Harmonics Program

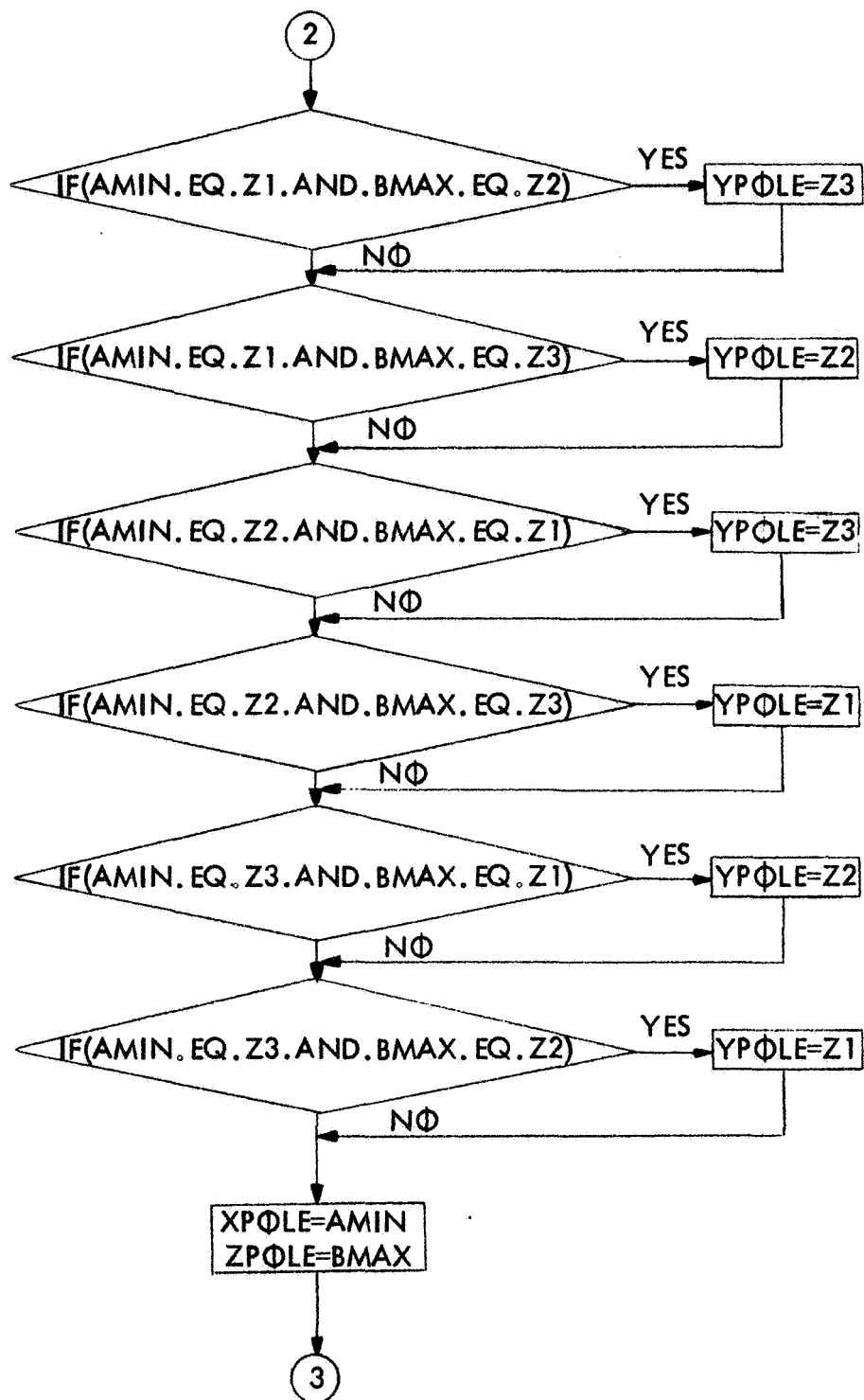


Table 4--Continued

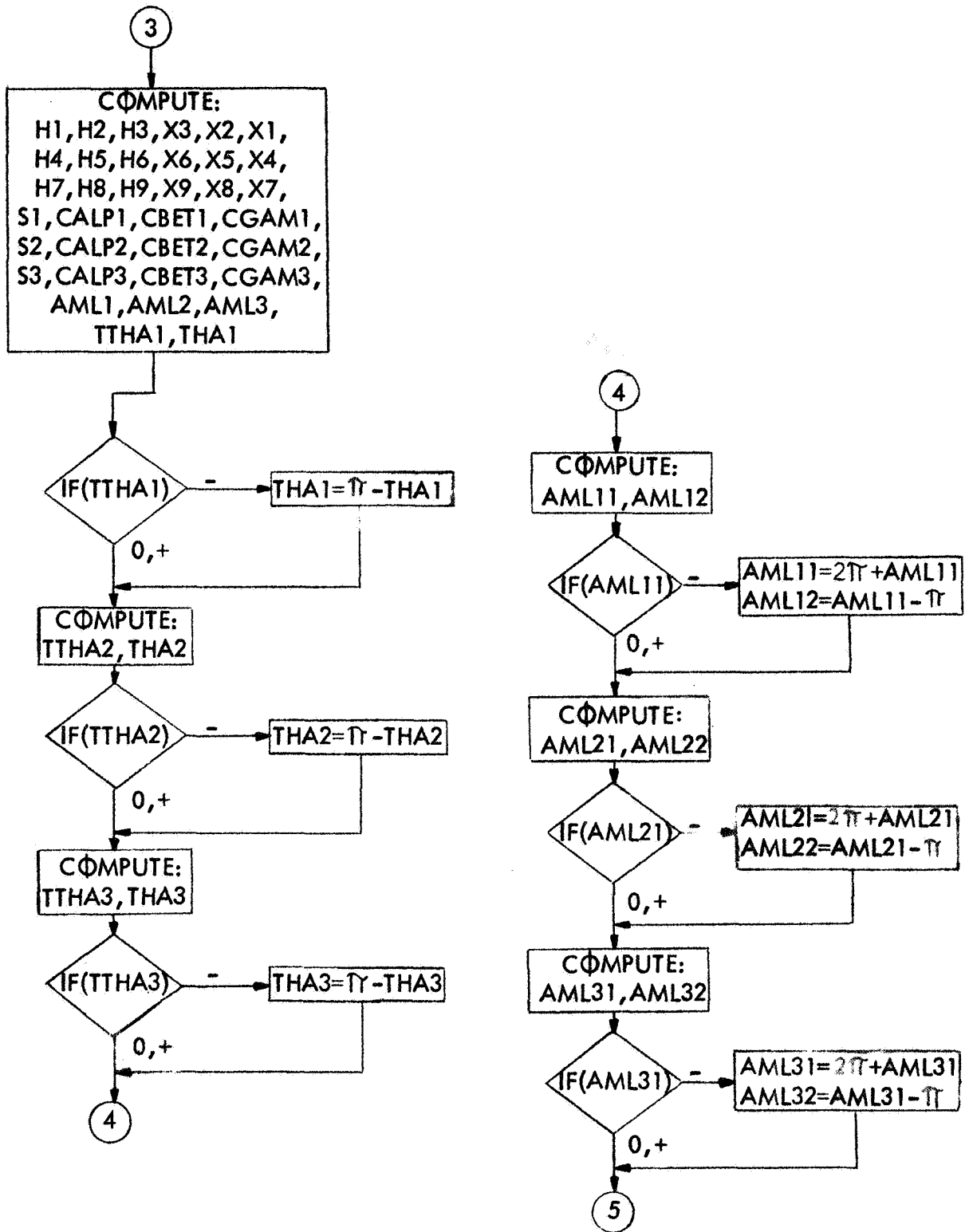


Table 4—Continued

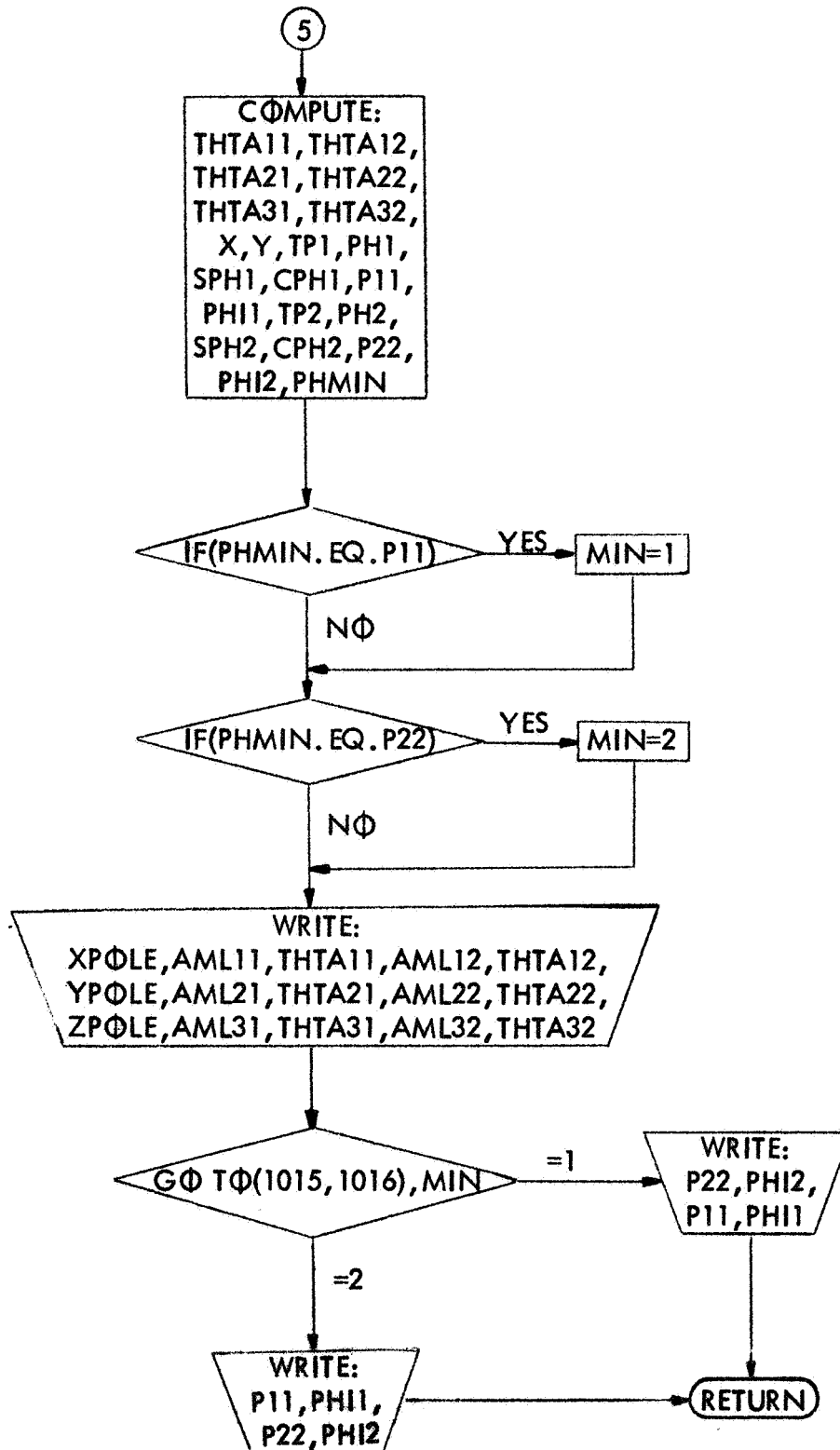


Table 4--Continued

```

C   SPHERICAL HARMONICS 10 DEGREE SQUARES
      DIMENSION THTA(19),SITA(19),COTA(19),ELAM( 37),B(18, 36),SM(19),F
      A19),COML( 37),SIML( 37),THP(18),APAL( 36),BPAL( 36),A(18, 36)
      COMMON F(18,36),RUN(18),CIS(4),SIS(4)
C NC=NO OF VALUES OF COLAT CONSIDERED, NL=NO OF EAST LONG
      ICCK=-1
      READ(5,7000) ICC
7000  FORMAT(I4)
3050  ICCK=ICCK+1
      IF(ICCK.EQ.ICC) CALL EXIT
      READ(5,2001) (RUN(ID),ID=1,18)
2001  FORMAT(18A4)
      READ(5,2003) NC,NL,NMN,IPRT,ITR
2003  FORMAT(5I4)
      READ(5,2033) ((F(I,J),J=1,NL),I=1,NC)
2033  FORMAT(18F4.2)
      IF(IPRT.EQ.1) CALL PRNT
      WRITE(6,2039)
2039  FORMAT(1H1,11X,35HCOEFFICIENTS OF SPHERICAL HARMONICS)
      WRITE(6,2040)
2040  FORMAT(1H0,11X,1HN,7X,1HM,9X,3HCNM,11X,3HSNM)
      NL1=NL+1
      NC1=NC+1
      NMNI=0
      ELCO=6.28318/FLOAT(NL)
      THCO=3.14159/FLOAT(NC)
      THTA(1)=0.
      ELAM(1)=0.
      SITA(1)=0.
      COTA(1)=1.
C FORM SERIES OF THETAS, LAMBDAS, SINES AND COSINES FOR P CALC.
      DO 100 I=2,NC1
        THTA(I)=THTA(I-1)+THCO
        SITA(I)=SIN(THTA(I))
100    COTA(I)=COS(THTA(I))
      DO 200 J=2,NL1
        ELAM(J)=ELAM(J-1)+ELCO
C FORM SUMMATION PART OF P, RELATED TO ACTUAL THETAS, WHEN R=0, SUBS=1
C GET VALUE OF M AND N, FORM ALL FACTORIALS, THEN SUM, THEN P
3000  READ(5,2028) N,M,ISTR
2028  FORMAT(3I4)
      LIM=N-M+1
      FISU=0.
      DO 400 I=1,NC1
        DO 500 L=1,LIM
          IF1=M+(L-1)
          IF(IF1.EQ.0) GO TO 1
          IFX1=1
          DO 2 II=1,IF1
            IFX1=IFX1*II
          F1=IFX1
104    IF2=N-(L-1)
          IF(IF2.EQ.0) GO TO 3
          IFX2=1
          DO 4 II=1,IF2
            IFX2=IFX2*II

```

Table 5--Listing of "MAIN" routine of Spherical Harmonics Program

```

F2=IFX2
106 IF3=N-M-(L-1)
    IF(IF3.EQ.0) GO TO 5
    IFX3=1
    DO 6 II=1,IF3
        6 IFX3=IFX3*II
        F3=IFX3
108 IF4=L-1
    IF(IF4.EQ.0) GO TO 7
    IFX4=1
    DO 8 II=1,IF4
        8 IFX4=IFX4*II
        F4=IFX4
    GO TO 9
    1 F1=1.
    GO TO 104
    3 F2=1.
    GO TO 106
    5 F3=1.
    GO TO 108
    7 F4=1.
    9 IF((N-M-(L-1)).EQ.0) GO TO 10
    IF((COTA(I)-1.).EQ.0.) GO TO 111
    Q=(COTA(I)-1.)*(N-M-(L-1))
    GO TO 11
111 Q=0.
    GO TO 11
    10 Q=1.
    11 IF((L-1).EQ.0) GO TO 12
    IF((COTA(I)+1.).EQ.0.) GO TO 112
    R=(COTA(I)+1.)*(L-1)
    GO TO 13
112 R=0.
    GO TO 13
    12 R=1.
    13 HASU=(Q*R)/(F1*F2*F3*F4)
    FISU=FISU+HASU
500 CONTINUE
C SUMMATION PART OF P NOW COMPLETE
    IF5=N-M
    IF(IF5.EQ.0) GO TO 14
    IFX5=1
    DO 15 II=1,IF5
        15 IFX5=IFX5*II
        F5=IFX5
110 IF6=N+M
    IF(IF6.EQ.0) GO TO 16
    IFX6=1
    DO 17 II=1,IF6
        17 IFX6=IFX6*II
        F6=IFX6
    GO TO 401
    14 F5=1.
    GO TO 110
    16 F6=1.
401 IF(M.EQ.0) GO TO 402

```

```

      IF(SITA(I).EQ.0.) GO TO 403
      SM(I)=SITA(I)**M
      GO TO 404
402  SM(I)=1.
      GO TO 404
403  SM(I)=0.
404  IF(N.EQ.0) GO TO 405
      TTN=2**N
      GO TO 406
405  TTN=1.
406  P(I)=F5*F6*SM(I)*FISU/TTN
      FISU=0.
400  CONTINUE
C ALL PS ARE CAL. AND STORED RELATIVE TO THETAS AT THIS POINT
      EM=M
      DO 600 J=1,NL1
        SIML(J)=SIN(EM*ELAM(J))
600  COML(J)=COS(EM*ELAM(J))
      DO 700 I=1,NC
700  THP(I)=(P(I)*SITA(I)+P(I+1)*SITA(I+1))/2.
      IF(M.EQ.0) GO TO 801
      DO 800 J=1,NL
        APAL(J)=(COML(J)+COML(J+1))/2.
800  BPAL(J)=(SIML(J)+SIML(J+1))/2.
      GO TO 901
801  DO 802 J=1,NL
        APAL(J)=1.
802  BPAL(J)=0.
901  DO 900 I=1,NC
      DO 900 J=1,NL
        A(I,J)=F(I,J)*THP(I)*APAL(J)*THCO*ELCO
900  B(I,J)=F(I,J)*THP(I)*BPAL(J)*THCO*ELCO
      IF(M.EQ.0) GO TO 21
      IF7=N
      IF(IF7.EQ.0) GO TO 18
      IFX7=1
      DO 19 II=1,IF7
19  IFX7=IFX7*II
      F7=IFX7
      GO TO 20
18  F7=1.
20  CONST=(FLOAT(2*N+1)*F7)/(6.28319*F6)
      GO TO 22
21  CONST=(FLOAT(2*N+1))/12.56636
22  CSUM=0.
      SSUM=0.
      DO 1000 I=1,NC
      DO 1000 J=1,NL
        CSUM=CSUM+A(I,J)
1000 SSUM=SSUM+B(I,J)
      CMN=CSUM*CONST
      SMN=SSUM*CONST
      WRITE(6,2041) N,M,CMN,SMN
2041 FORMAT(1H0,10X,12,6X,12,4X,1PE12.5,3X,1PE12.5)
      IF(ISTR.EQ.0) GO TO 3020
      CIS(ISTR)=CMN

```

```
SIS(ISTR)=SMN  
3020 NMNI=NMNI+1  
IF(NMNI.EQ.NMN.AND. ITR .EQ.1) CALL TENS  
IF(NMNI.EQ.NMN) GO TO 3050  
GO TO 3000  
END
```

```

SUBROUTINE PRNT
C   SPHERICAL HARMONICS 10 DEGREE SQUARES
COMMON F(18,36),RUN(18),CIS(4),SIS(4)
2005 FORMAT(1H ,10X,1H0)
2006 FORMAT(1H ,9X,2H10)
2007 FORMAT(1H ,9X,2H20)
2008 FORMAT(1H ,9X,2H30)
2009 FORMAT(1H ,9X,2H40)
2025 FORMAT(1H ,5X,1HC,7X,9(F4.2,2X))
2010 FORMAT(1H ,5X,1H0,3X,2H50)
2026 FORMAT(1H ,5X,1HL,7X,9(F4.2,2X))
2011 FORMAT(1H ,5X,1HA,3X,2H60)
2027 FORMAT(1H ,5X,1HT,7X,9(F4.2,2X))
2012 FORMAT(1H ,5X,1HI,3X,2H70)
2013 FORMAT(1H ,5X,1HU,3X,2H80)
2029 FORMAT(1H ,5X,1HD,7X,9(F4.2,2X))
2014 FORMAT(1H ,5X,1HE,3X,2H90)
2030 FORMAT(1H ,13X,9(F4.2,2X))
2015 FORMAT(1H ,5X,1H-,2X,3H100)
2016 FORMAT(1H ,5X,1HT,2X,3H110)
2031 FORMAT(1H ,5X,1HH,7X,9(F4.2,2X))
2017 FORMAT(1H ,5X,1HE,2X,3H120)
2018 FORMAT(1H ,5X,1HA,2X,3H130)
2019 FORMAT(1H ,8X,3H140)
2020 FORMAT(1H ,8X,3H150)
2021 FORMAT(1H ,8X,3H160)
2022 FORMAT(1H ,8X,3H170)
2023 FORMAT(1H ,8X,3H180)
WRITE(6,2002)(RUN(ID),ID=1,17)
2002 FORMAT(1H1,17A4)
WRITE(6,2034)
2034 FORMAT(1H0,28X,22HEAST LONGITUDE - LAMDA)
WRITE(6,2035)
2035 FORMAT(1H0,12X,1H0,4X,2H10,4X,2H20,4X,2H30,4X,2H40,4X,2H50,4X,2H
A,4X,2H70,4X,2H80,4X,2H90)
WRITE(6,2005)
WRITE(6,2030) (F(1,I),I=1,9)
WRITE(6,2006)
WRITE(6,2030) (F(2,I),I=1,9)
WRITE(6,2007)
WRITE(6,2030) (F(3,I),I=1,9)
WRITE(6,2008)
WRITE(6,2030) (F(4,I),I=1,9)
WRITE(6,2009)
WRITE(6,2025) (F(5,I),I=1,9)
WRITE(6,2010)
WRITE(6,2026) (F(6,I),I=1,9)
WRITE(6,2011)
WRITE(6,2027) (F(7,I),I=1,9)
WRITE(6,2012)
WRITE(6,2027) (F(8,I),I=1,9)
WRITE(6,2013)
WRITE(6,2029) (F(9,I),I=1,9)
WRITE(6,2014)
WRITE(6,2030) (F(10,I),I=1,9)
WRITE(6,2015)

```

Table 6—Listing of "PRNT" subroutine of Spherical Harmonics Program

```

WRITE(6,2030) (F(11,1),I=1,9)
WRITE(6,2016)
WRITE(6,2031) (F(12,1),I=1,9)
WRITE(6,2017)
WRITE(6,2027) (F(13,1),I=1,9)
WRITE(6,2018)
WRITE(6,2030) (F(14,1),I=1,9)
WRITE(6,2019)
WRITE(6,2030) (F(15,1),I=1,9)
WRITE(6,2020)
WRITE(6,2030) (F(16,1),I=1,9)
WRITE(6,2021)
WRITE(6,2030) (F(17,1),I=1,9)
WRITE(6,2022)
WRITE(6,2030) (F(18,1),I=1,9)
WRITE(6,2023)
WRITE(6,2002) (RUN(10),I0=1,17)
WRITE(6,2034)
WRITE(6,2036)
2036 FORMAT(1H0,11X,2H90,3X,3H100,3X,3H110,3X,3H120,3X,3H130,3X,3H140,
1X,3H150,3X,3H160,3X,3H170,3X,3H180)
WRITE(6,2005)
WRITE(6,2030) (F(1,1),I=10,18)
WRITE(6,2006)
WRITE(6,2030) (F(2,1),I=10,18)
WRITE(6,2007)
WRITE(6,2030) (F(3,1),I=10,18)
WRITE(6,2008)
WRITE(6,2030) (F(4,1),I=10,18)
WRITE(6,2009)
WRITE(6,2025) (F(5,1),I=10,18)
WRITE(6,2010)
WRITE(6,2026) (F(6,1),I=10,18)
WRITE(6,2011)
WRITE(6,2027) (F(7,1),I=10,18)
WRITE(6,2012)
WRITE(6,2027) (F(8,1),I=10,18)
WRITE(6,2013)
WRITE(6,2029) (F(9,1),I=10,18)
WRITE(6,2014)
WRITE(6,2030) (F(10,1),I=10,18)
WRITE(6,2015)
WRITE(6,2030) (F(11,1),I=10,18)
WRITE(6,2016)
WRITE(6,2031) (F(12,1),I=10,18)
WRITE(6,2017)
WRITE(6,2027) (F(13,1),I=10,18)
WRITE(6,2018)
WRITE(6,2030) (F(14,1),I=10,18)
WRITE(6,2019)
WRITE(6,2030) (F(15,1),I=10,18)
WRITE(6,2020)
WRITE(6,2030) (F(16,1),I=10,18)
WRITE(6,2021)
WRITE(6,2030) (F(17,1),I=10,18)
WRITE(6,2022)

```

```

WRITE(6,2030) (F(18,I),I=10,18)
WRITE(6,2023)
WRITE(6,2002) (RUN(ID),ID=1,17)
WRITE(6,2034)
WRITE(6,2037)
2037 FORMAT(1H0,10X,3H180,3X,3H190,3X,3H200,3X,3H210,3X,3H220,3X,3H23
13X,3H240,3X,3H250,3X,3H260,3X,3H270)
WRITE(6,2005)
WRITE(6,2030) (F(1,I),I=19,27)
WRITE(6,2006)
WRITE(6,2030) (F(2,I),I=19,27)
WRITE(6,2007)
WRITE(6,2030) (F(3,I),I=19,27)
WRITE(6,2008)
WRITE(6,2030) (F(4,I),I=19,27)
WRITE(6,2009)
WRITE(6,2025) (F(5,I),I=19,27)
WRITE(6,2010)
WRITE(6,2026) (F(6,I),I=19,27)
WRITE(6,2011)
WRITE(6,2027) (F(7,I),I=19,27)
WRITE(6,2012)
WRITE(6,2027) (F(8,I),I=19,27)
WRITE(6,2013)
WRITE(6,2029) (F(9,I),I=19,27)
WRITE(6,2014)
WRITE(6,2030) (F(10,I),I=19,27)
WRITE(6,2015)
WRITE(6,2030) (F(11,I),I=19,27)
WRITE(6,2016)
WRITE(6,2031) (F(12,I),I=19,27)
WRITE(6,2017)
WRITE(6,2027) (F(13,I),I=19,27)
WRITE(6,2018)
WRITE(6,2030) (F(14,I),I=19,27)
WRITE(6,2019)
WRITE(6,2030) (F(15,I),I=19,27)
WRITE(6,2020)
WRITE(6,2030) (F(16,I),I=19,27)
WRITE(6,2021)
WRITE(6,2030) (F(17,I),I=19,27)
WRITE(6,2022)
WRITE(6,2030) (F(18,I),I=19,27)
WRITE(6,2023)
WRITE(6,2002) (RUN(ID),ID=1,17)
WRITE(6,2034)
WRITE(6,2038)
2038 FORMAT(1H0,10X,3H270,3X,3H280,3X,3H290,3X,3H300,3X,3H310,3X,3H320
13X,3H330,3X,3H340,3X,3H350,3X,3H360)
WRITE(6,2005)
WRITE(6,2030) (F(1,I),I=28,36)
WRITE(6,2006)
WRITE(6,2030) (F(2,I),I=28,36)
WRITE(6,2007)
WRITE(6,2030) (F(3,I),I=28,36)
WRITE(6,2008)

```

```
WRITE(6,2030) (F(4,I),I=28,36)
WRITE(6,2009)
WRITE(6,2025) (F(5,I),I=28,36)
WRITE(6,2010)
WRITE(6,2026) (F(6,I),I=28,36)
WRITE(6,2011)
WRITE(6,2027) (F(7,I),I=28,36)
WRITE(6,2012)
WRITE(6,2027) (F(8,I),I=28,36)
WRITE(6,2013)
WRITE(6,2029) (F(9,I),I=28,36)
WRITE(6,2014)
WRITE(6,2030) (F(10,I),I=28,36)
WRITE(6,2015)
WRITE(6,2030) (F(11,I),I=28,36)
WRITE(6,2016)
WRITE(6,2031) (F(12,I),I=28,36)
WRITE(6,2017)
WRITE(6,2027) (F(13,I),I=28,36)
WRITE(6,2018)
WRITE(6,2030) (F(14,I),I=28,36)
WRITE(6,2019)
WRITE(6,2030) (F(15,I),I=28,36)
WRITE(6,2020)
WRITE(6,2030) (F(16,I),I=28,36)
WRITE(6,2021)
WRITE(6,2030) (F(17,I),I=28,36)
WRITE(6,2022)
WRITE(6,2030) (F(18,I),I=28,36)
WRITE(6,2023)
RETURN
END
```

```

SUBROUTINE TENSr
C  TENSOR OF INERTIA
COMMON F(18,36),RUN(18),CIS(4),SIS(4)
C00=CIS(1)
C20=CIS(2)
C21=CIS(3)
C22=CIS(4)
S21=SIS(3)
S22=SIS(4)
2  FORMAT(1H ,76HTEST OF Q**3+P**2 YIELDS A POSITIVE VALUE - ONE REAL
1  AND TWO IMAGINARY ROOTS)
3  FORMAT(1H ,58H R IS NEGATIVE, CALCULATION STOPPED, RETURN TO MAIN P
1ROGRAM)
PRINT 1000
1000 FORMAT(1H1,31HSpherical HARMONIC COEFFICIENTS)
PRINT 1001
1001 FORMAT(1H0,7X,3HC00,7X,3HC20,7X,3HC21,7X,3HC22,7X,3HS21,7X,3HS22)
1002 FORMAT(1H, 2X,6(3X,F7.4),/)
WRITE(6,1002) C00,C20,C21,C22,S21,S22
EM1=C20
EM2=4.*C22+C20
EM3=2.*C22
EM4=2.*S22
EM5=C21
EM6=S21
101 PRINT 90
90  FORMAT(1H0,15HMATRIX ELEMENTS)
PRINT 91
91  FORMAT(1H0,7X,3HM11,7X,3HM22,7X,3HM33,5X,7HM12=M21,3X,7HM13=M31,3X
1,7HM23=M32)
WRITE(6,1002) EM1,EM2,EM3,EM4,EM5,EM6
PRINT 107
107 FORMAT(1H0,62HPRINCIPAL MOMENTS EAST LONG COLATITUDE EAST LONG
1COLATITUDE)
PRINT 108
108 FORMAT(1H ,60H OF INERTIA (DEG) (DEG) (DEG)
1 (DEG) )
A=1.
B=- (EM1+EM2+EM3)/3.
C=- (-EM1*EM2-EM1*EM3-EM2*EM3+EM4**2+EM5**2+EM6**2)/3.
D=- (EM1*EM2*EM3+2.*EM4*EM5*EM6-EM1*EM6**2-EM2*EM5**2-EM3*EM4**2)
Q=A*C-P**2
R=.5*(3.*A*B*C-A**2*D)-B**3
TEST=Q**3+R**2
IF (TEST) 12,13,14
14 PRINT 2
GO TO 32
13 SI=R**(1./3.)
Z1=(2.*SI-D)/A
Z2=(-SI-B)/A
Z3=Z2
XPOLE=AMIN1(Z1,Z2)
ZPOLE=AMAX1(Z1,Z2)
YPOLE=ZPOLE
GO TO 199
12 P=ABS(R)/SQRT(-Q**3)

```

Table 7--Listing of "TENSr" subroutine of Spherical Harmonics Program

```

PART=ATAN(SQRT(1.-P**2)/P)/3.
IF(R) 15,16,17
16 PRINT 3
GO TO 32
15 COFF=-2.*SQRT(-Q)
GO TO 102
17 COEF=2.*SQRT(-Q)
102 Y1=COEF*COS(PART)
Y2=COEF*COS(PART+2.094395)
Y3=COEF*COS(PART+4.18879)
Z1=(Y1-B)/A
Z2=(Y2-B)/A
Z3=(Y3-B)/A
19 AMIN=AMIN1(Z1,Z2,Z3)
BMAX=AMAX1(Z1,Z2,Z3)
IF(AMIN.EQ.Z1.AND.BMAX.EQ.Z2) YPOLE=Z3
IF(AMIN.EQ.Z1.AND.BMAX.EQ.Z3) YPOLE=Z2
IF(AMIN.EQ.Z2.AND.BMAX.EQ.Z1) YPOLE=Z3
IF(AMIN.EQ.Z2.AND.BMAX.EQ.Z3) YPOLE=Z1
IF(AMIN.EQ.Z3.AND.BMAX.EQ.Z1) YPOLE=Z2
IF(AMIN.EQ.Z3.AND.BMAX.EQ.Z2) YPOLE=Z1
XPOLE=AMIN
ZPOLE=BMAX
199 H1=EM1-XPOLE
H2=EM2-XPOLE
H3=EM3-XPOLE
X3=(-EM5+EM4*EM6/H2)/(H3-EM6**2/H2)
X2=(-EM4-EM6*X3)/H2
X1=1.0
H4=EM1-YPOLE
H5=EM2-YPOLE
H6=EM3-YPOLE
X6=(-EM5+EM4*EM6/H5)/(H6-EM6**2/H5)
X5=(-EM4-EM6*X6)/H5
X4=1.0
H7=EM1-ZPOLE
H8=EM2-ZPOLE
H9=EM3-ZPOLE
X9=(-EM5+EM4*EM6/H8)/(H9-EM6**2/H8)
X8=(-EM4-EM6*X9)/H8
X7=1.0
S1=SQRT(X1**2+X2**2+X3**2)
CALP1=X1/S1
CBET1=X2/S1
CGAM1=X3/S1
S2=SQRT(X4**2+X5**2+X6**2)
CALP2=X4/S2
CBET2=X5/S2
CGAM2=X6/S2
S3=SQRT(X7**2+X8**2+X9**2)
CALP3=X7/S3
CBET3=X8/S3
CGAM3=X9/S3
AML1=ATAN2(CBET1,CALP1)
AML2=ATAN2(CBET2,CALP2)
AML3=ATAN2(CBET3,CALP3)

```

```

TTHA1=SQRT(1.-CGAM1**2)/CGAM1
THA1=ATAN(ABS(TTHA1))
IF(TTHA1) 26,27,27
26 THA1=3.141593-THA1
27 TTHA2=SQRT(1.-CGAM2**2)/CGAM2
THA2=ATAN(ABS(TTHA2))
IF(TTHA2) 28,29,29
28 THA2=3.141593-THA2
29 TTHA3=SQRT(1.-CGAM3**2)/CGAM3
THA3=ATAN(ABS(TTHA3))
IF(TTHA3) 30,31,31
30 THA3=3.141593-THA3
31 AML11=57.29578*AML1
AML12=180.+AML11
IF(AML11) 33,34,34
33 AML11=360.+AML11
AML12=AML11-180.
34 AML21=57.29577*AML2
AML22=180.+AML21
IF(AML21) 35,36,36
35 AML21=360.+AML21
AML22=AML21-180.
36 AML31=57.29578*AML3
AML32=180.+AML31
IF(AML31) 37,38,38
37 AML31=360.+AML31
AML32=AML31-180.
38 THTA11=57.29578*THA1
THTA12=180.-THTA11
THTA21=57.29578*THA2
THTA22=180.-THTA21
THTA31=57.29578*THA3
THTA32=180.-THTA31
X=C22/S22
Y=SQRT(X**2+1.)
TP1=X+Y
PH1=ATAN(TP1)
SPH1=SIN(PH1)
CPH1=COS(PH1)
P11=(C00+.1*C20)/3.+(.1*C22*(SPH1**2-CPH1**2)+.2*S22*SPH1*CPH1)/2
PH11=57.29578*PH1
TP2=X-Y
PH2=3.141593-ATAN(ABS(TP2))
SPH2=SIN(PH2)
CPH2=COS(PH2)
P22=(C00+.1*C20)/3.+(.1*C22*(SPH2**2-CPH2**2)+.2*S22*SPH2*CPH2)/2
PH12=57.29578*PH2
PHMIN=AMIN1(P11,P22)
IF(PHMIN.EQ.P11) MIN=1
IF(PHMIN.EQ.P22) MIN=2
WRITE(6,1010) XPOLE,AML11,THTA11,AML12,THTA12
WRITE(6,1011) YPOLE,AML21,THTA21,AML22,THTA22
WRITE(6,1012) ZPOLE,AML31,THTA31,AML32,THTA32
1010 FORMAT(1H0,5H X ,F8.5,3X,4(3X,F8.3))
1011 FORMAT(1H0,5H Y ,F8.5,3X,4(3X,F8.3))
1012 FORMAT(1H0,5H Z ,F8.5,3X,4(3X,F8.3))

```

```
      PRINT 1013
1013 FORMAT(1H0,31HMOMENT OF INERTIA IN  EAST LONG)
      PRINT 1014
1014 FORMAT(1H ,29H EQUATORIAL PLANE      (DEG))
      GO TO (1015,1016),MIN
1015 WRITE(6,1017) P22,PHI2
1017 FORMAT(1H0,7H MAX ,F8.5,8X,F8.3)
      WRITE(6,1019) P11,PHI1
1019 FORMAT(1H0,7H MIN ,F8.5,8X,F8.3)
      RETURN
1016 WRITE(6,1017) P11,PHI1
      WRITE(6,1019) P22,PHI2
32   RETURN
      END
```

Table 8--Symbols Used in "MAIN" Routine of Moon Modeling Program

Fortran Nomenclature	Explanation
Variables	
CNMP	$\left. \begin{matrix} c_{n,m'} \\ s_{n,m'} \end{matrix} \right\}$ coefficients of spherical harmonic representation of the distribution of surface features
SNMP	
HI	differences in elevation between maria and continents; and between circular basins and areas outside of basins
TITLE	label for identification
CNM	$\left. \begin{matrix} c_{n,m} \\ s_{n,m} \end{matrix} \right\}$ coefficients of a surface spherical harmonic expansion of the gravity field
SNM	
EN	n
CPT	$d_{n,m} = \frac{(2n+1)c_{n,m}}{c_{n,m'}}$
HC	$H = d_{n/m} \frac{1738.}{3.}$
SPT	$d_{n,m} = \frac{(2n+1)s_{n,m}}{s_{n,m'}}$
HS	$H = d_{n,m} \frac{1738.}{3.}$
Integers	
N	n
M	m
IMAX	number of n,m combinations considered
J	counter for the distributions considered (4)
K	counter for the sets of data considered (3)
L	counter for HI
LMAX	number of HI considered

Table 9--Symbols Used in "COMPT" subroutine of Moon Modeling Program

Fortran Nomenclature	Explanation
Variables	
A	radius of moon
R1	$\rho_a$ , average density of moon
R2	$\rho_i$ , density of nickel-iron
R3	$\rho_{mm}$ , density of material beneath maria or circular basins
R4	$\rho_c$ , density of crustal material
H	HI (see "MAIN" explanation)
T	t, thickness of nickel-iron layer
DELRA	$\Delta\rho(a)$ , density contrast
X	} intermediate storage locations for quadratic calculation of additional density contrasts
Y	
Z	
SQQ	
SQ	
D	depth of compensation
DRA	$\Delta\rho(a)$ , density contrast
Integers	
L	counter for HI
LMAX	number of HI considered